Met Office

The challenge of applying consistent ice optical properties and microphysics in climate models

Anthony J. Baran (Met Office & University of Hertfordshire), James Manners (Met Office), Kalli Furtado (Met Office), Paul Field (Met Office & Leeds University), Peter Hill (University of Reading), Odran Sourdeval (University of Lille), Joseph (Ulanowski, University of Hertfordshire), Thomas Blackmore (Met Office)

FORUM workshop, Florence, Italy, October 2018

Contents

- The importance of the far-ir spectrum and cirrus to the prediction of weather & climate
- Why we need more observations from across the spectrum to constrain NWP & climate models
- The ensemble model of cirrus ice crystals and its parametrisation via a coupled microphysics-radiation approach
- The impact of the coupled parametrisation in the MO's next Earth System model relative to the control model & CERES global SW & LW observations at TOA via coupled ocean-atmosphere simulations
- Uncertainties that will affect the far-ir and our interpretations of its usefulness to constrain cirrus models
- Discussion

Met Office

The importance of the far-ir and cirrus in model prediction of weather and climate

Contributions of the far-ir to the total outgoing long-wave radiation

Edwards-Slingo calculations show that TOA flux ratio Far-ir/total-ir

15 μm < λ < 125 μm

Tropics ~ 42% (new light scattering observations from the TTL)
Mid-Lat Winter/Summer ~ 50%/44%
Sub-arctic Winter/Summer ~ 54%/45%

~50% of IR radiation exits Earth's atmosphere via the far-ir

Consistent with previous findings in the literature

The importance of cirrus in weather and climate prediction

Met Office

Weighted towards simple ice crystals **in the PSDs**

Same PSDs but weighted towards more aggregated ice crystals

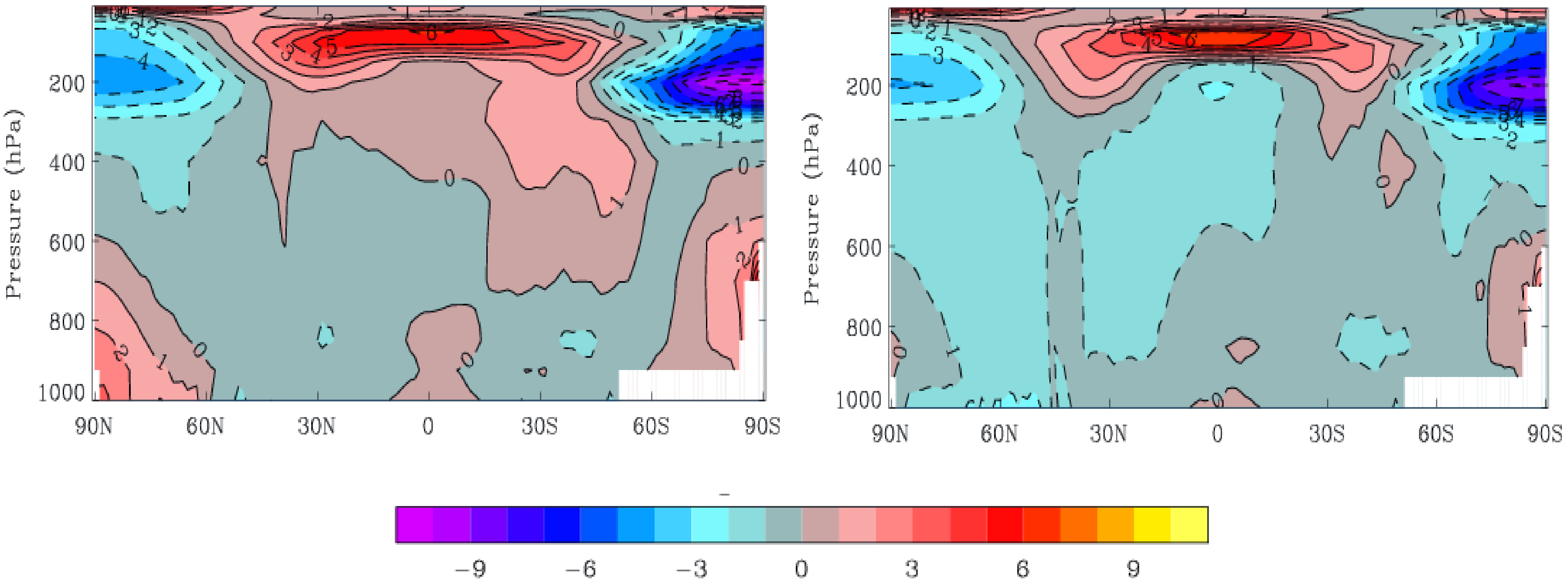

Model minus ERA-Interim temperature product

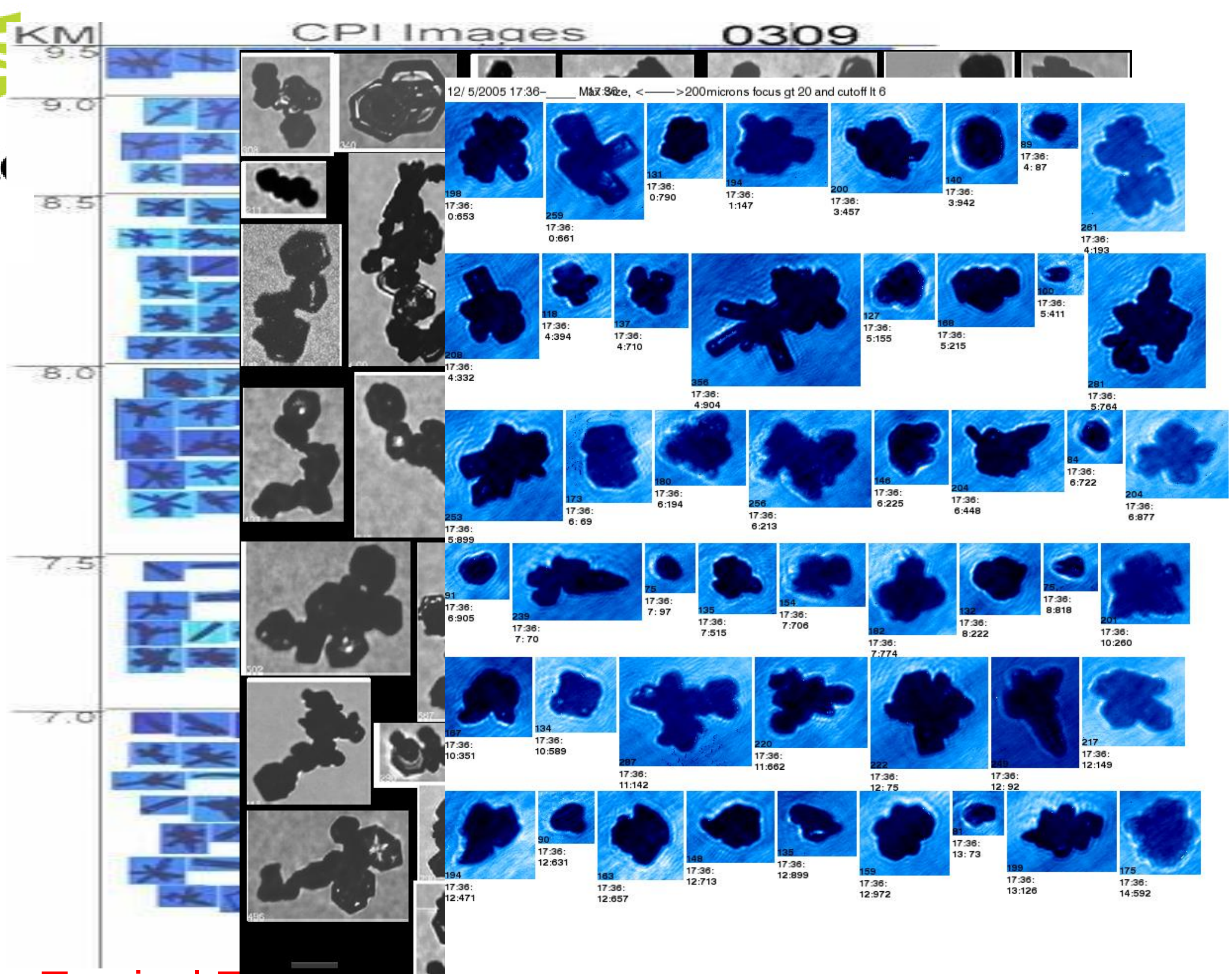

Tropical Example, A Heymsfield

University of Manchester

2008.

The A-Train Constellation measures radiative properties & ice mass

Total & polarized solar reflection

94 GHz cloud-profiling radar

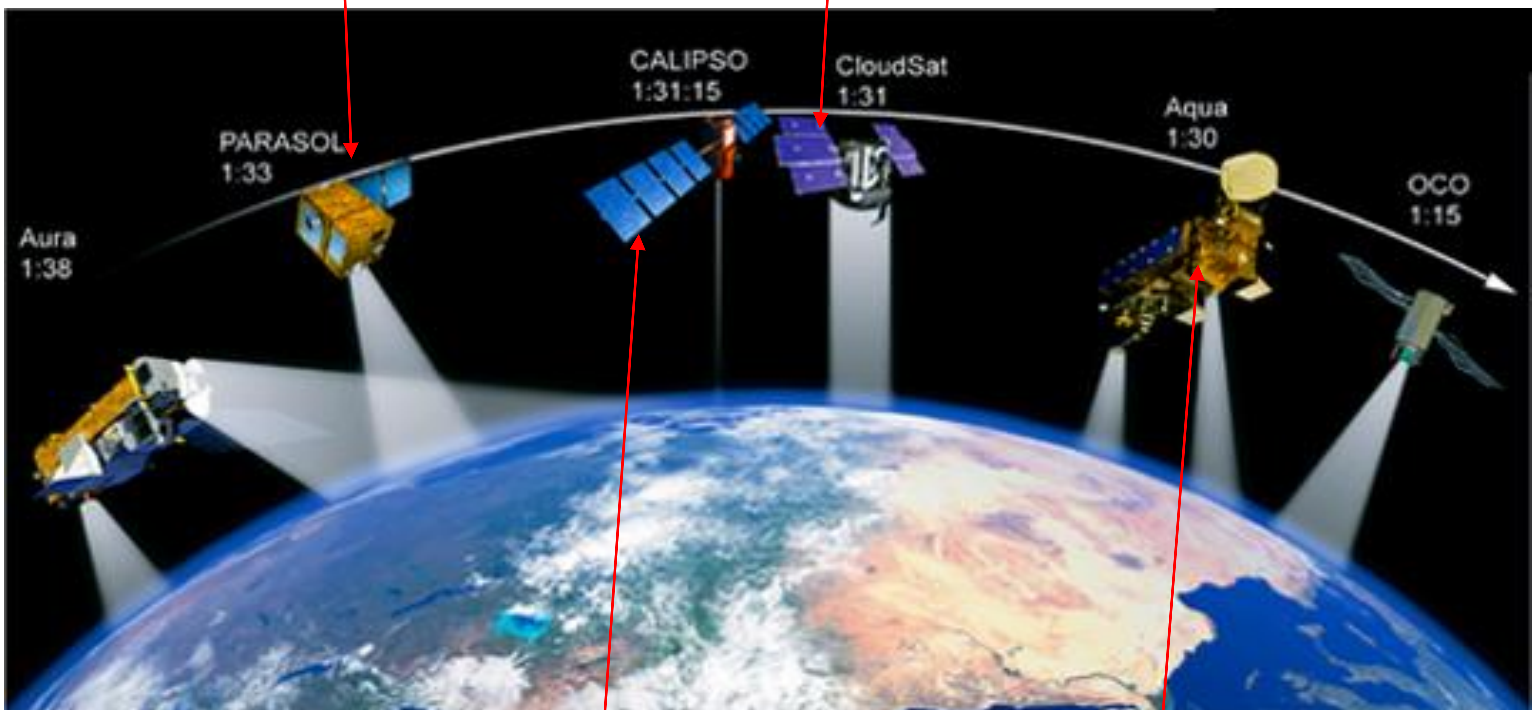

2020s Ice Cloud imager (mm & sub-mm) – FORUM ??

Lidar

Solar reflection & Infrared transmission

Met Office

THE ENSEMBLE MODEL OF CIRRUS ICE CRYSTALS

Generalise

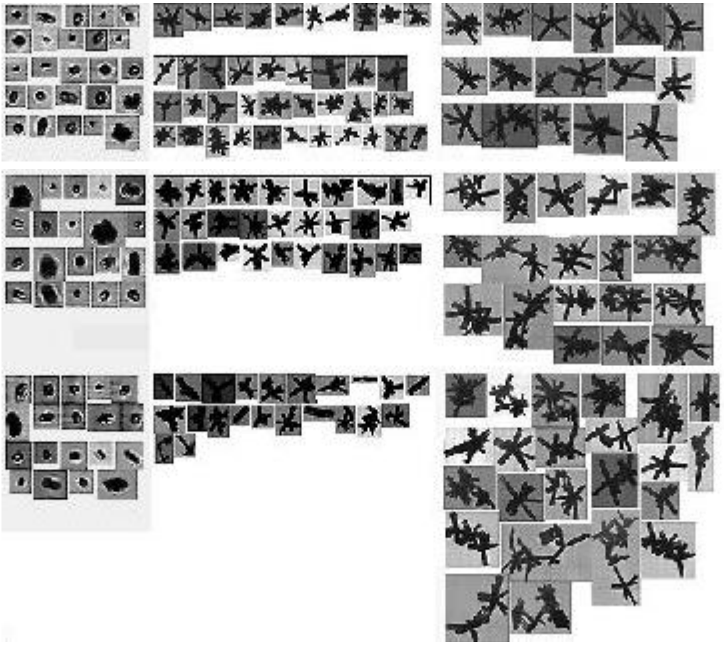

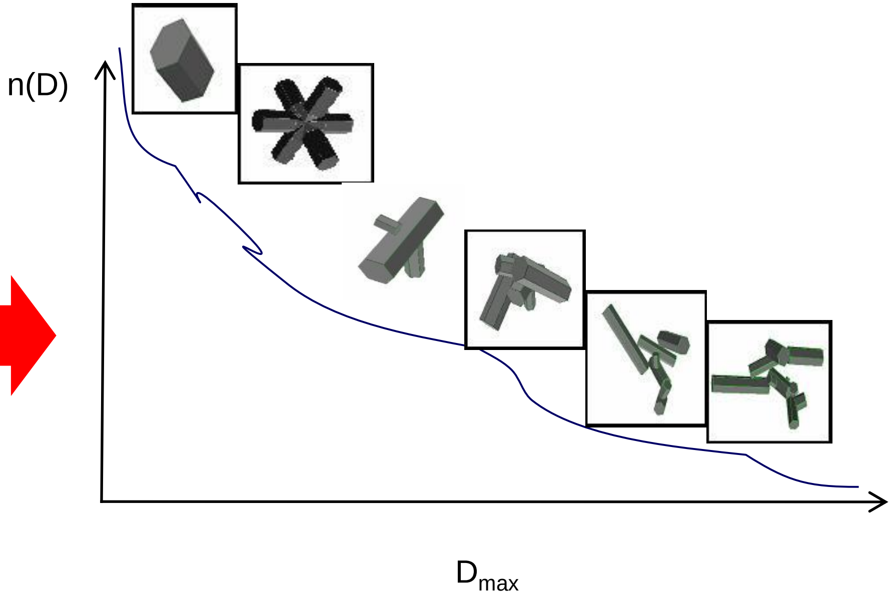

Baran & Labonnote (2007)

Microphysical Consistency

Observed area Relationships: Area ratio:

$A(D)/A_c(D)$

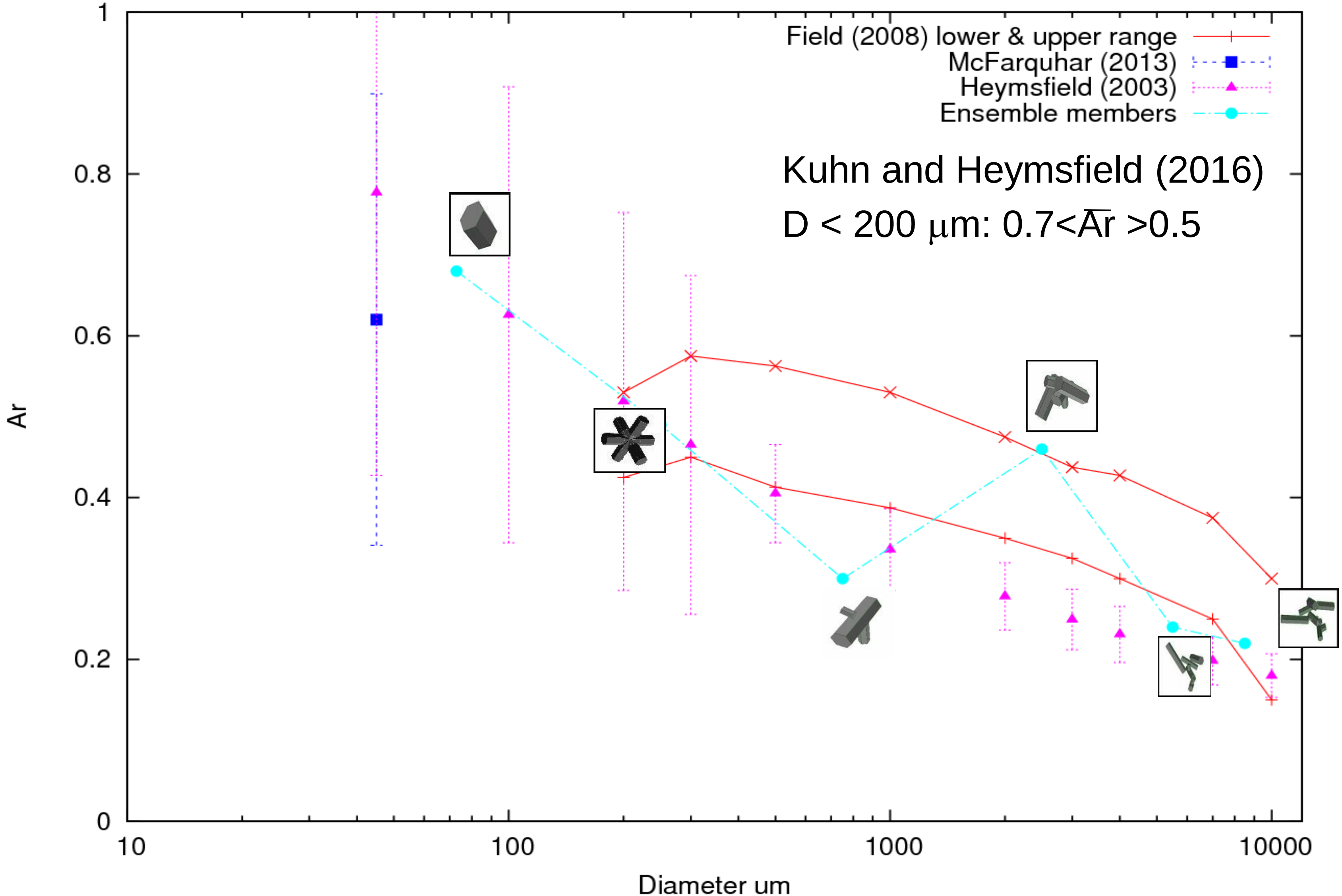

Moment estimation parameterization, Field et al. (2007)

$$M_n = \int D^n f(D)\, dD,\ n \geq 0$$

$$M_n = \alpha_n \exp(\sigma_n T_c) M_2^{\beta_n}$$

$$M_2 = aD^{b=2},\ a = 0.0257 \text{ (Cotton et al., 2013)}$$

Links PSD to ice mass and T_c. Moments are used to predict cloud evolution

PSDs in climate model cloud microphysics scheme same as radiation scheme & mass-D relationship same in both to generate PSDs

We apply tropical normalisation

To obtain bulk cirrus scattering properties

IWC, T_c

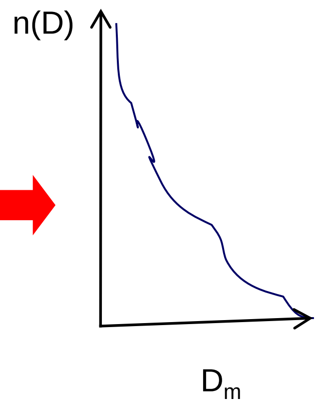

Field et al. 2007

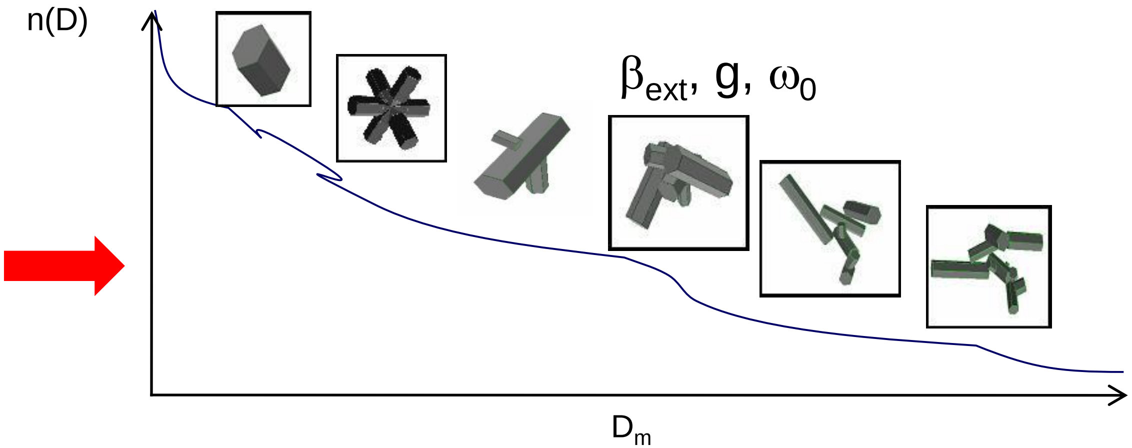

$$\langle \beta_{ext} \rangle = \int_{D_{min}}^{D_{max}} n(D) \left[\sum_{j=1}^{j=6} wt_j \langle C_{ext_j} \rangle \right] dD$$

IWC (Closure)

Same PSDs as in cirrus microphysics

Bulk K_{ext}, g, ω_0

Directly related to IWC, T_c

Baran et al. 2009

Ensemble model phase functions

Baran et al. 2015

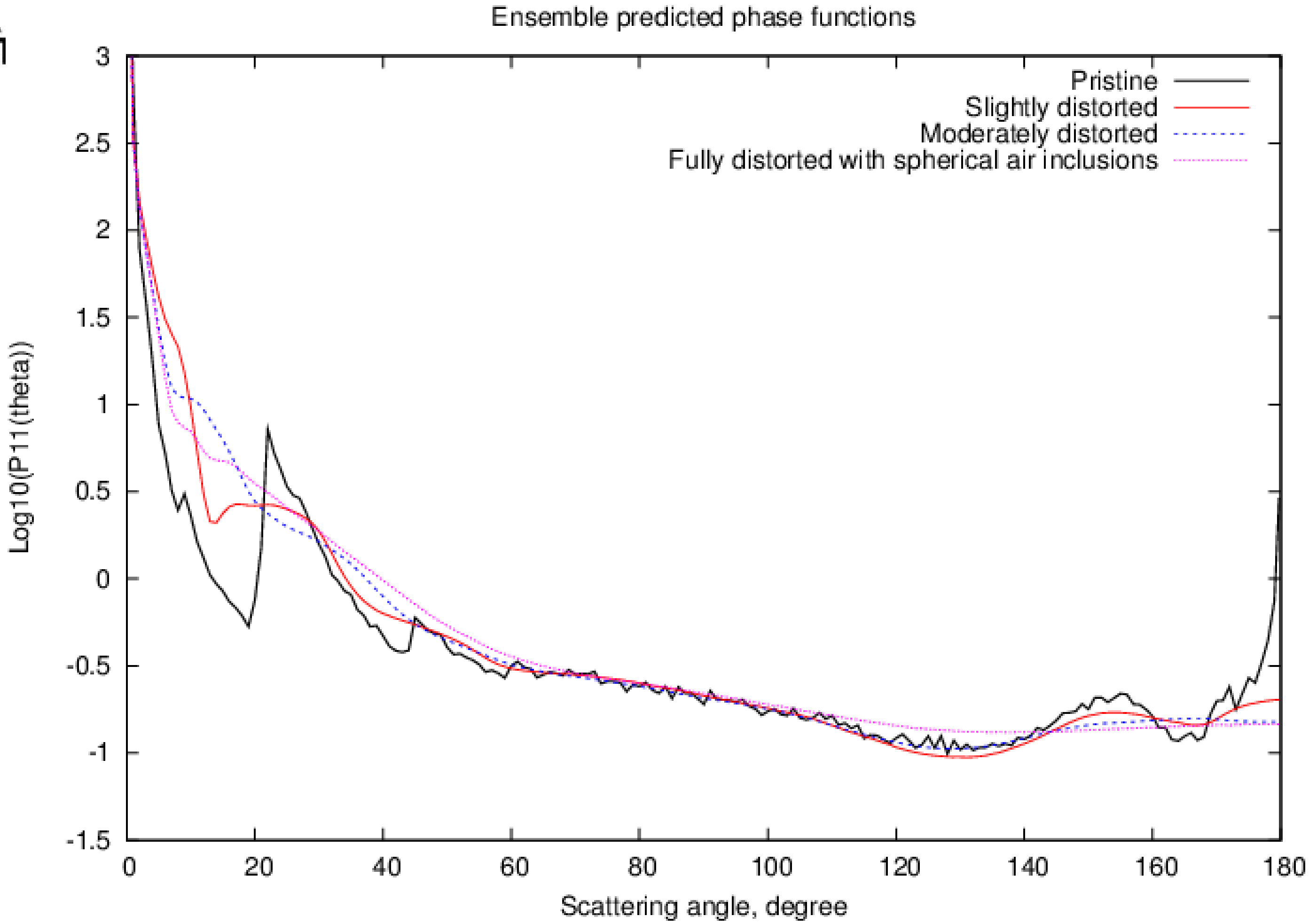

New experimental evidence of ice crystal complexity and featureless phase functions

Dataset of ~10 000 single particle angular scattering phase functions with a stereo image. For each figure 1,2,5,10,50 or 100 single particle angular scattering functions are averaged 100 times.

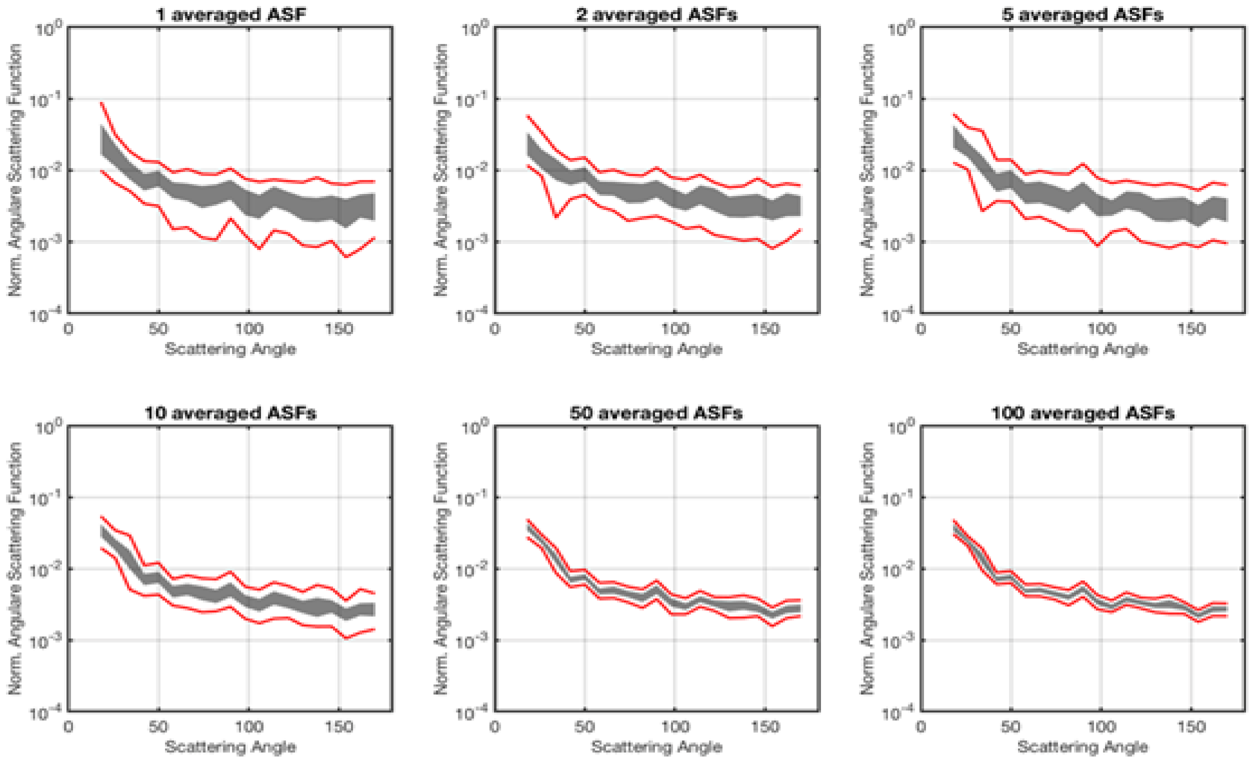

From Jarvinen et al. AMS, Vancouver July 2018

ω_0 and g in M_2-T_C space: λ=1.575 µm

$K_{ext}(\lambda_{E\text{-}S},q_i,T_c)$, $\omega_0(\lambda_{E\text{-}S},q_i,T_c)$, $g(\lambda_{E\text{-}S},q_i,T_c)$ Baran et al. (2016)

wt_j= 0.50 0.20 0.30

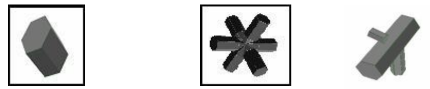

ω_0 g

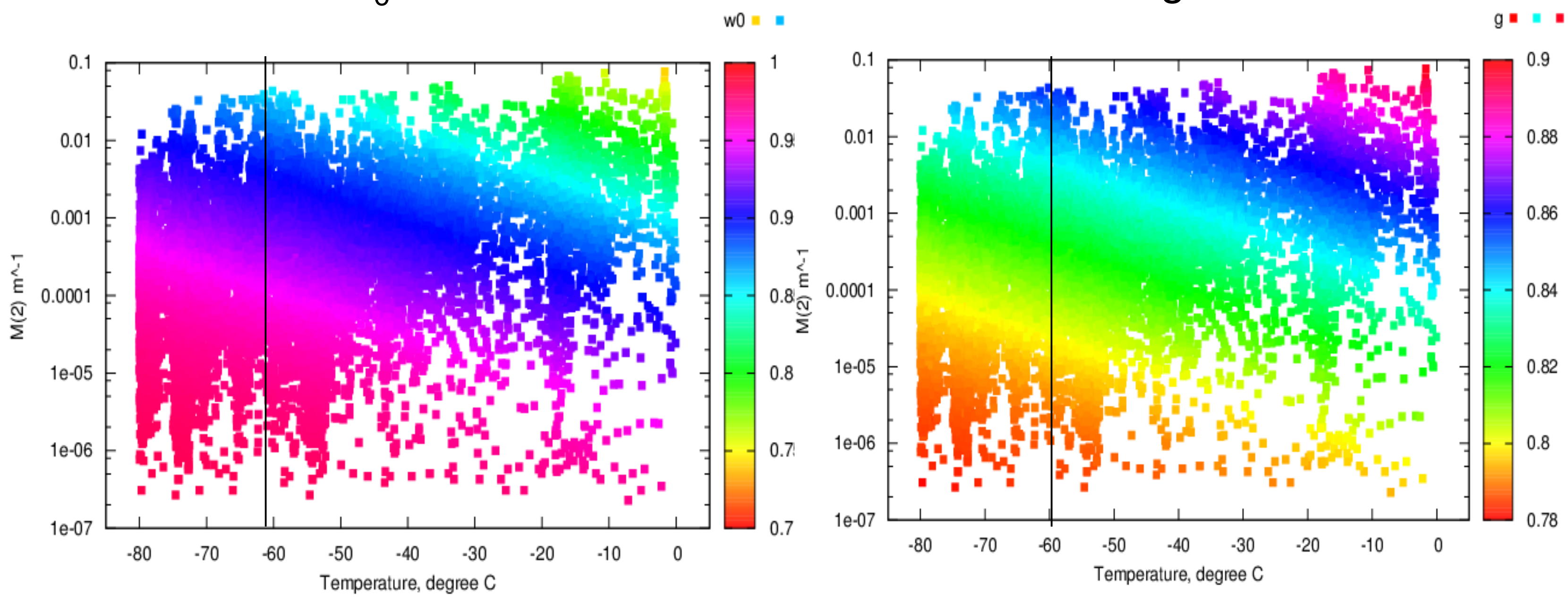

Baran et al. (2016)

The IWC and cloud temperature were obtained from a number of field campaigns including CAESAR (UK), CEPEX (Tropics), FRAMZY (Europe)

A total number of 20662 PSDs were generated & randomly generated

The impact of the ice optics parametrisation in GA 7 relative to observations & the previous parametrisation

Met Office

Annual 20-year TOA area-averaged annual mean of coupled ocean-atmosphere model minus CERES EBAF SW reflection and OLR

Inconsistent model GC2 | Consistent model (GC3) next CMIP

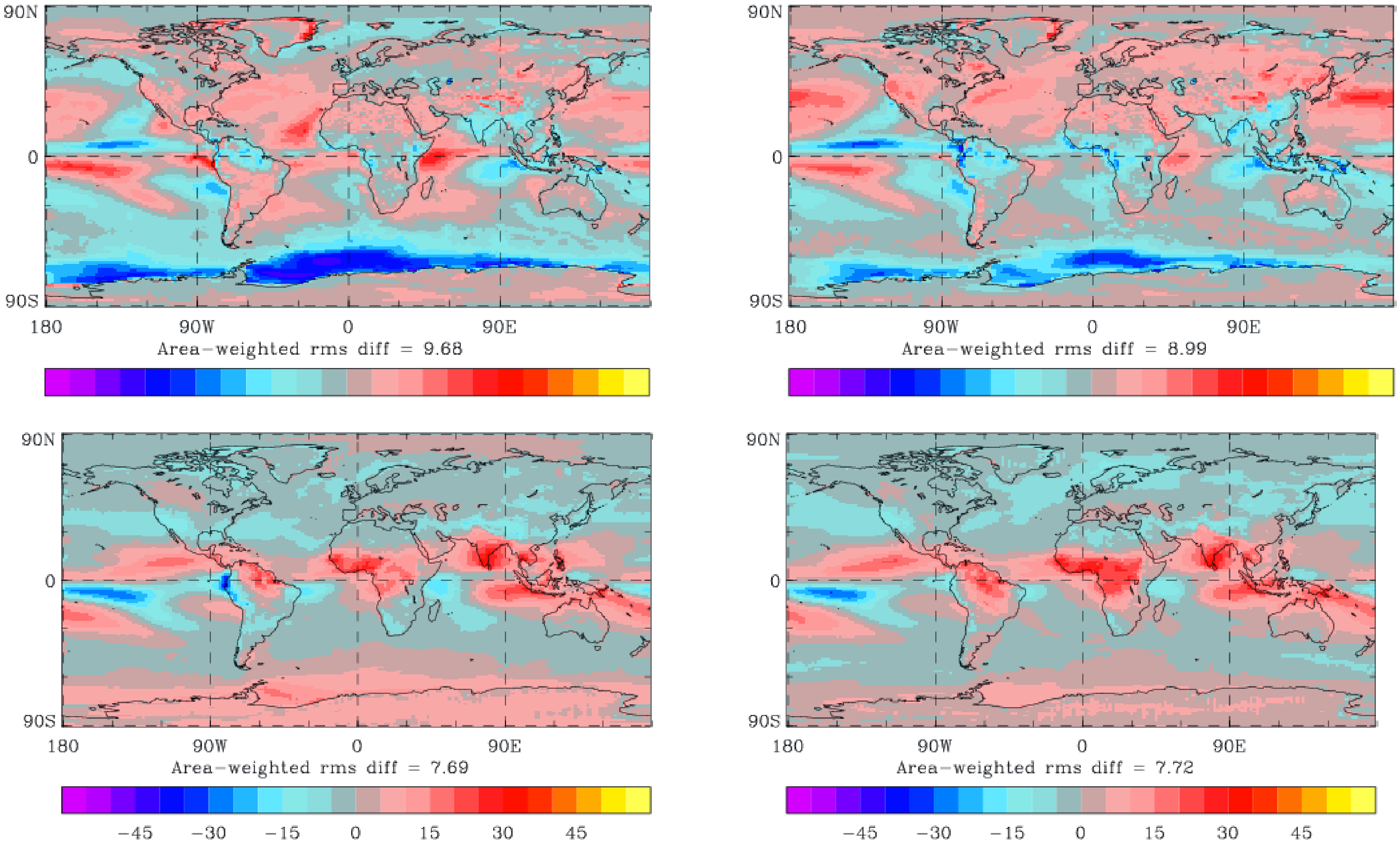

10.8 μm

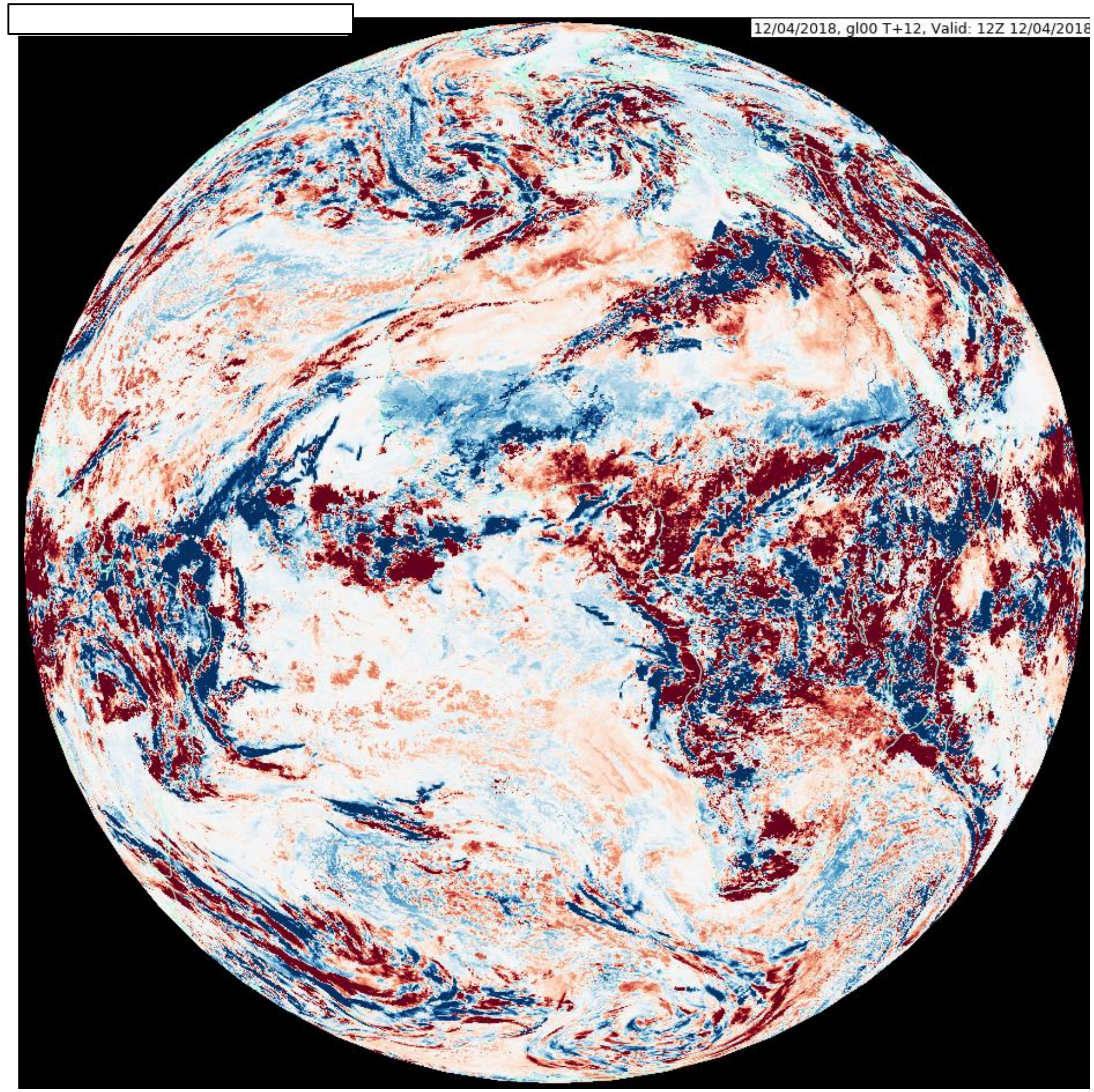

Observations minus Model
(Baran scheme)

NWP simulation using
RTTOV – fast model

10.8 μm

Observations minus Model (SSEC/Wisconsin, ide=4)

NWP simulation using RTTOV – fast model

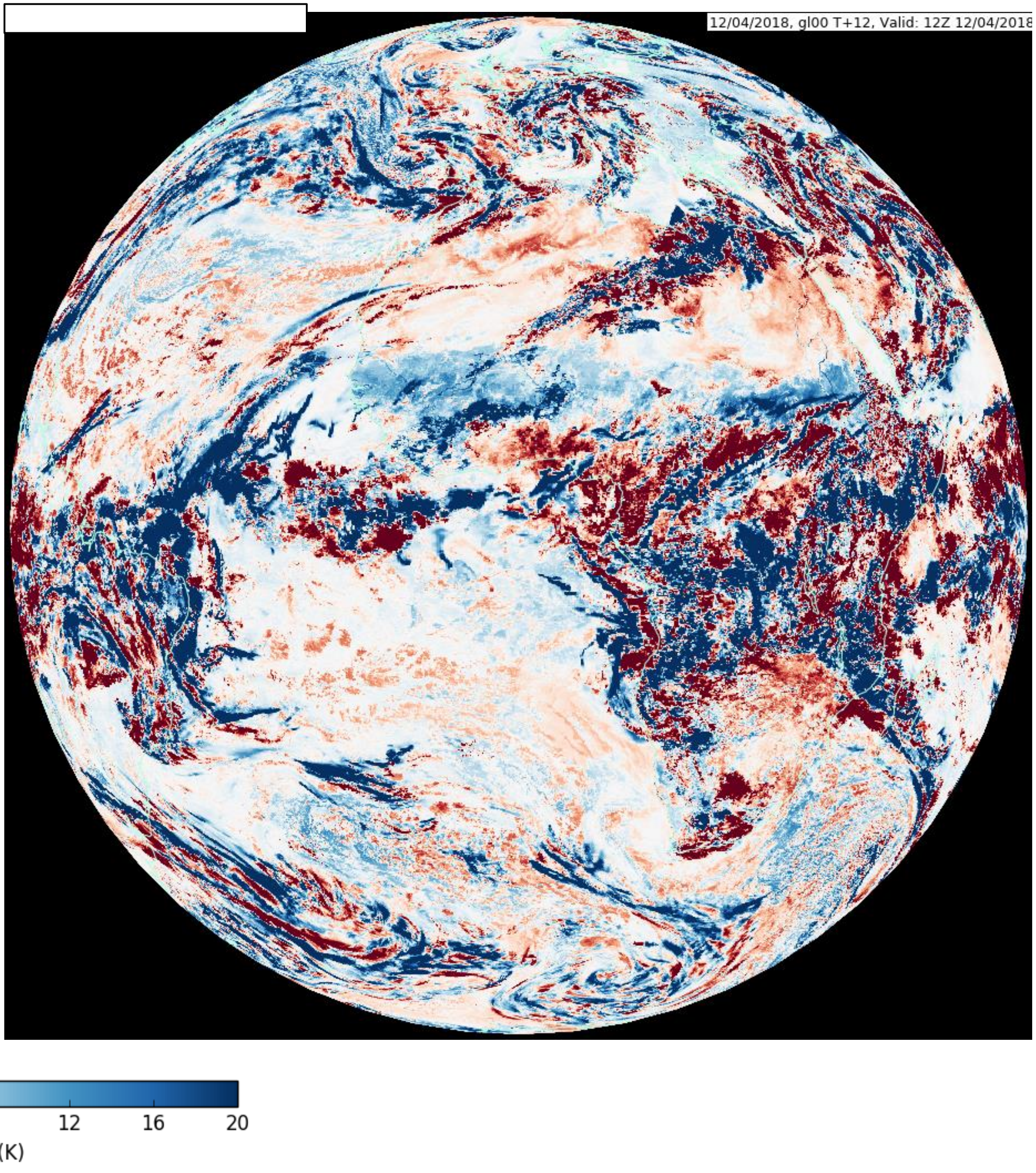

Uncertainties that will impact on the far-ir

Comparison of PSD parametrisations against in-situ measured PSDs (From ATTREX and SPARTICUS)

SPARTICUS

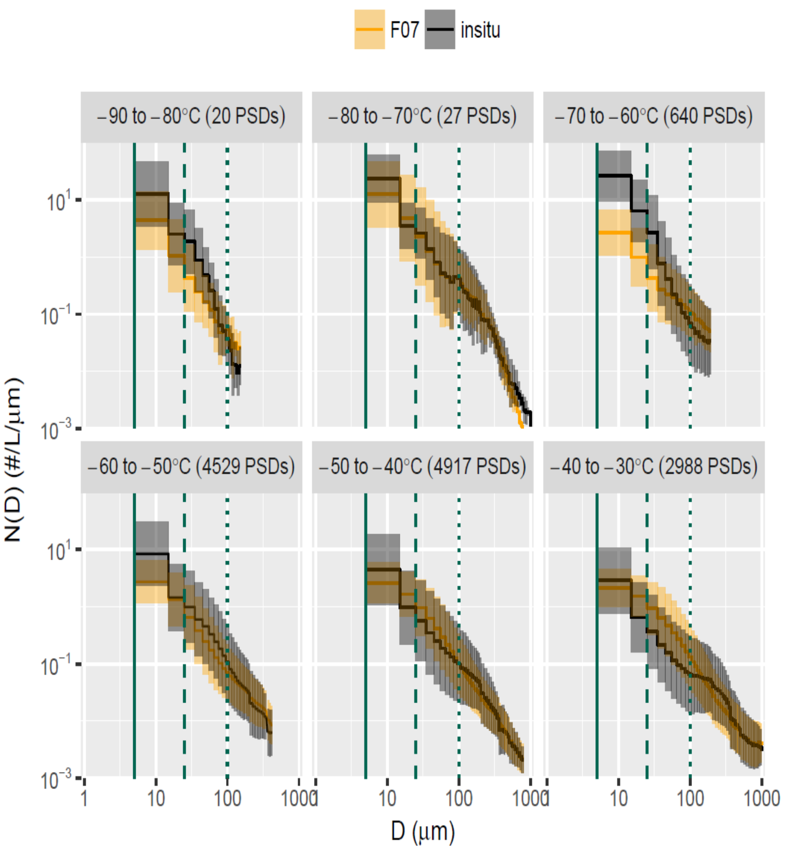

ATTREX – TTL

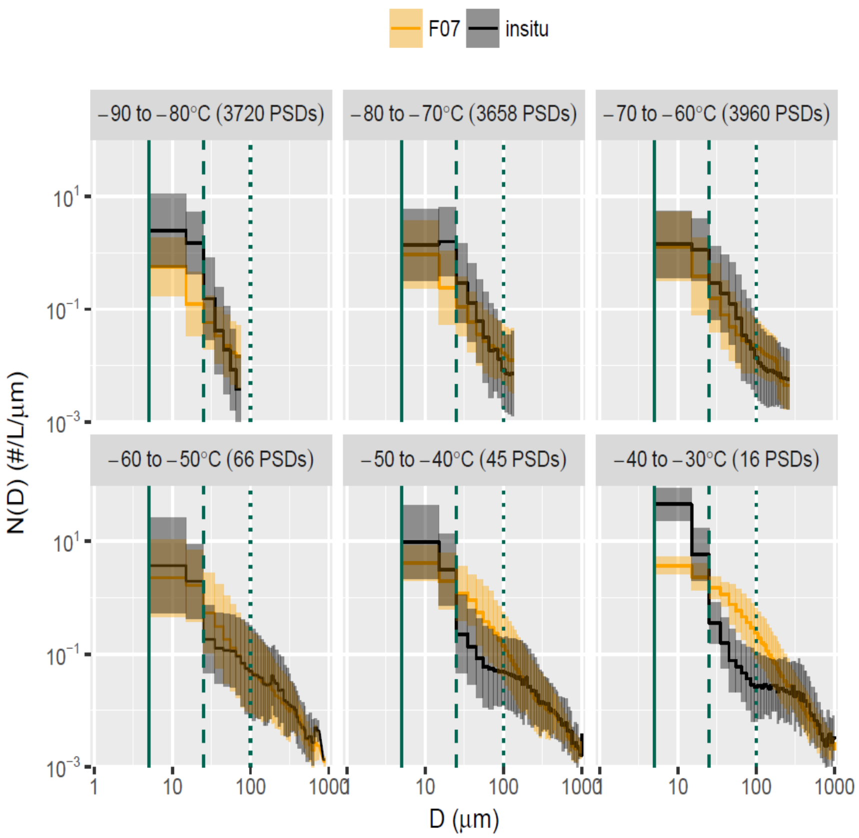

Courtesy of Odran Sourdeval (University of Leipzig)

Which shape of the small ice mode?

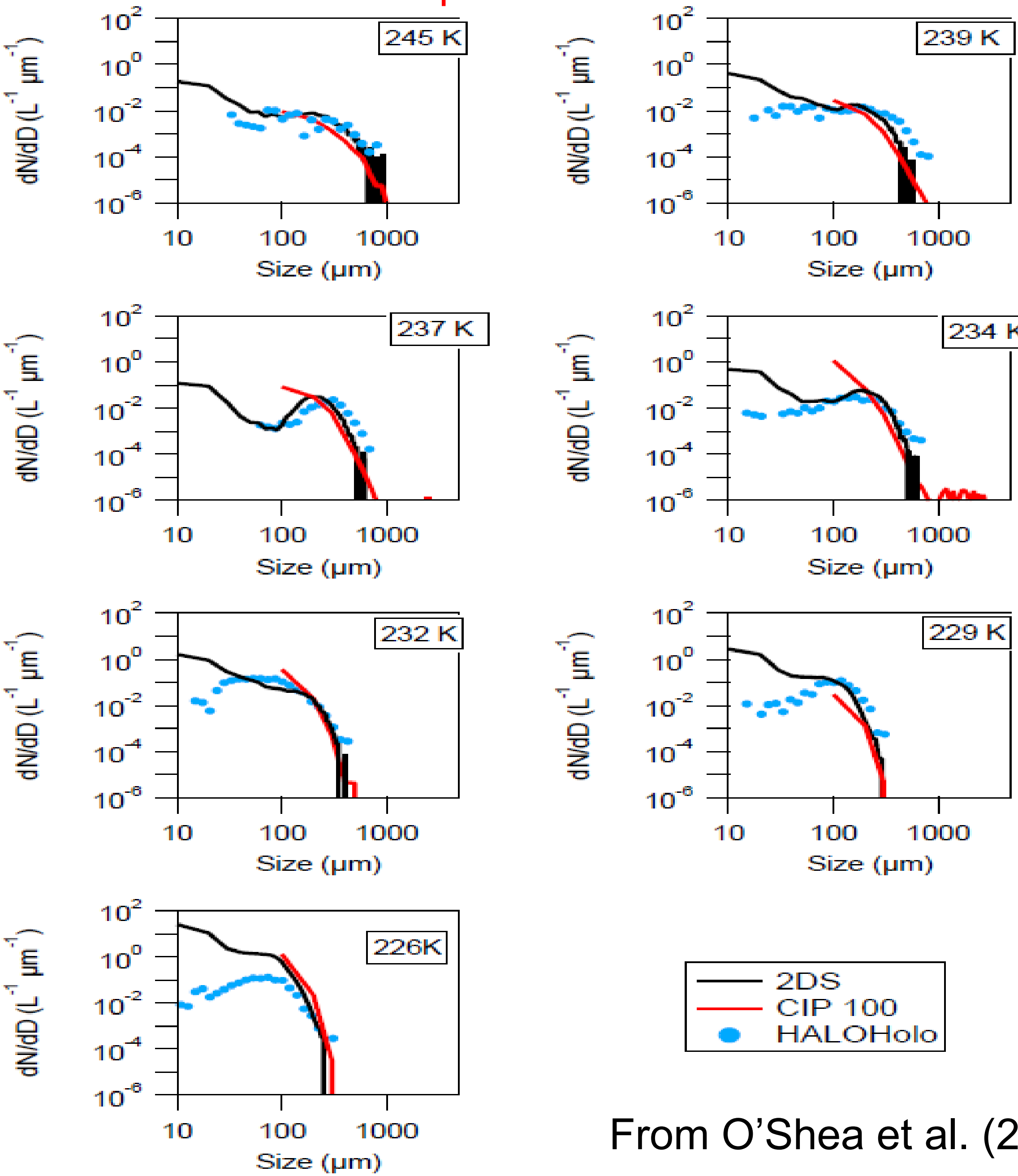

From O'Shea et al. (2016), Fig 5a

PSD small ice uncertainty: which shape of the small ice mode?

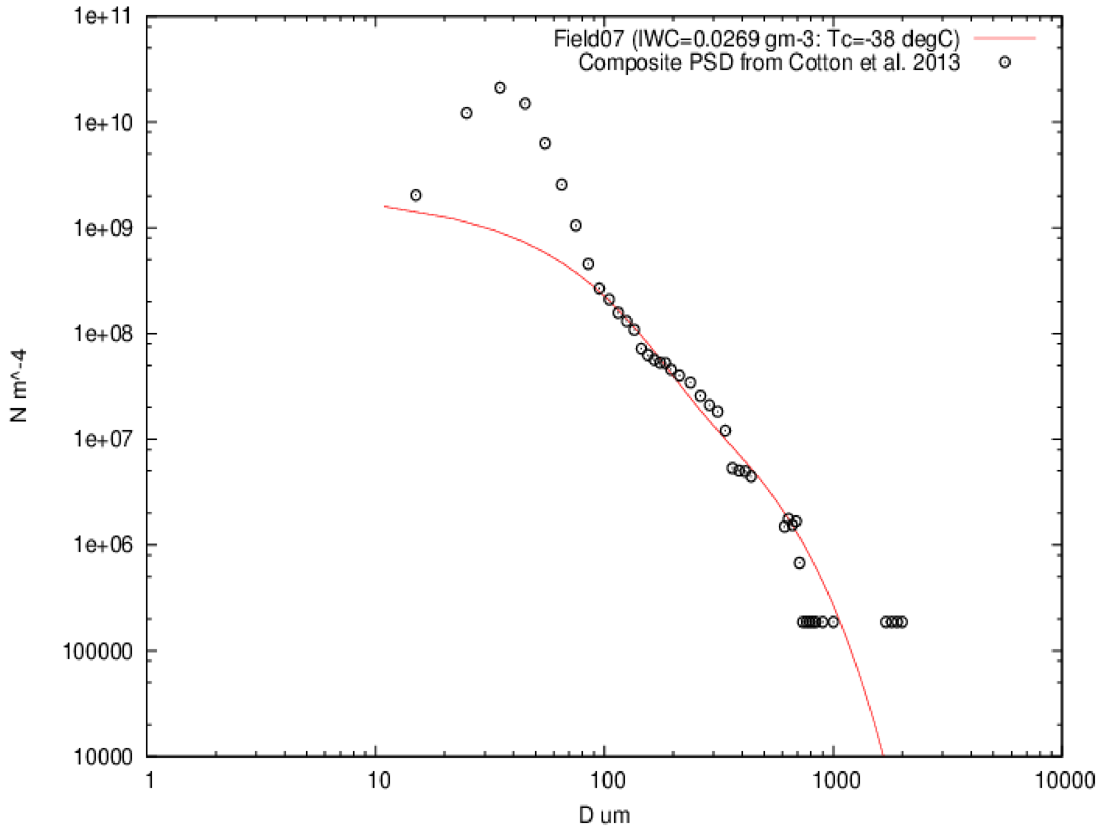

The effect of small ice uncertainty on absorptivity

Absorption

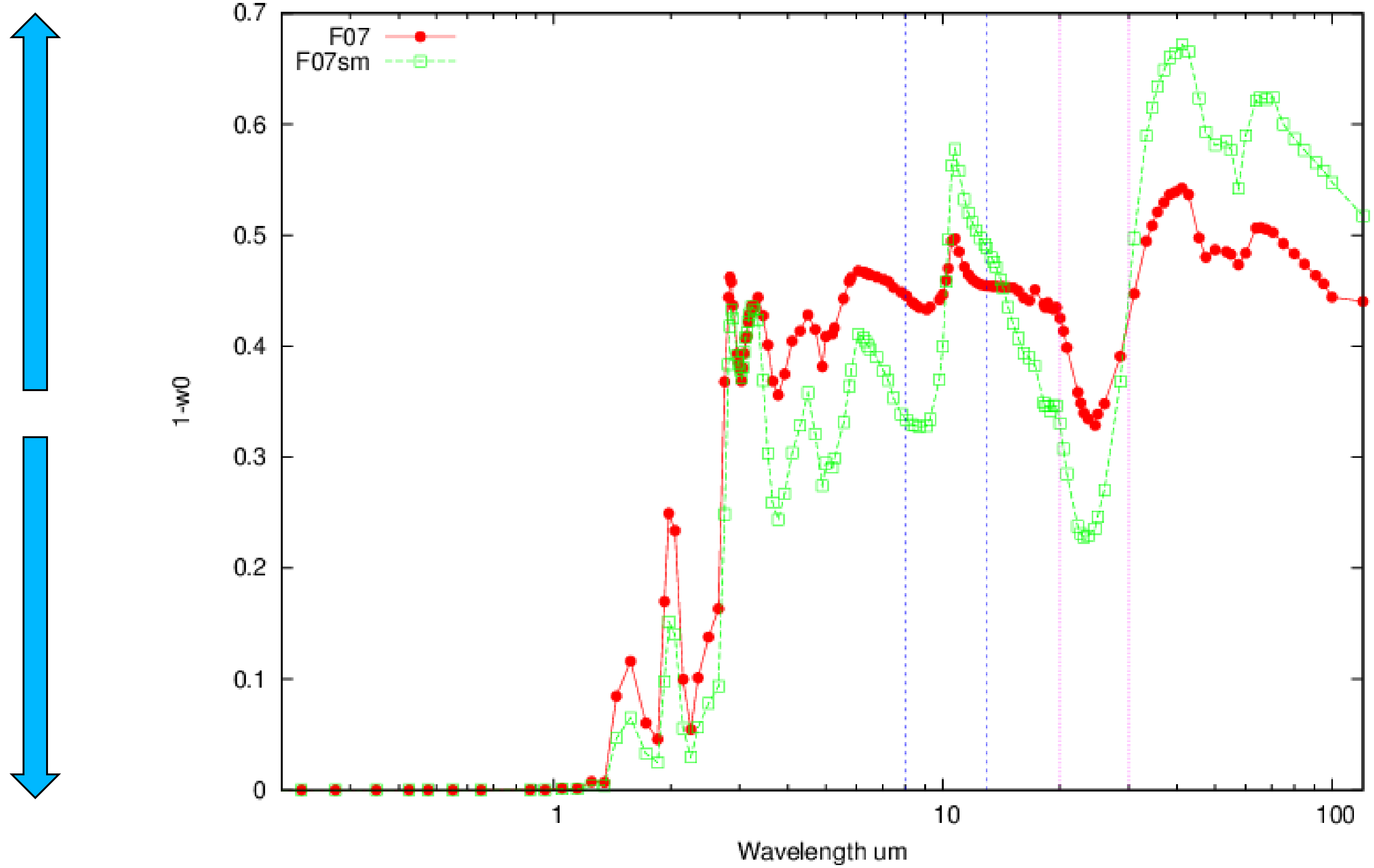

Scattering

SID3 – 2D patterns

Mid-latitude cirrus and mixed phase clouds, CONSTRAIN

University of Hertfordshire

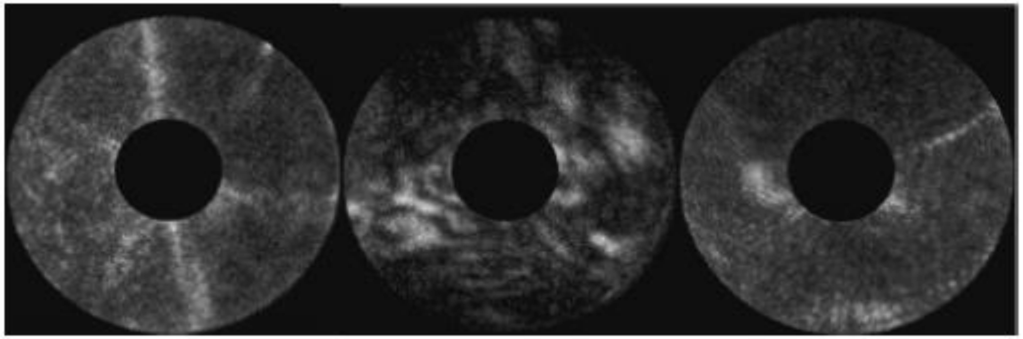

cirrus

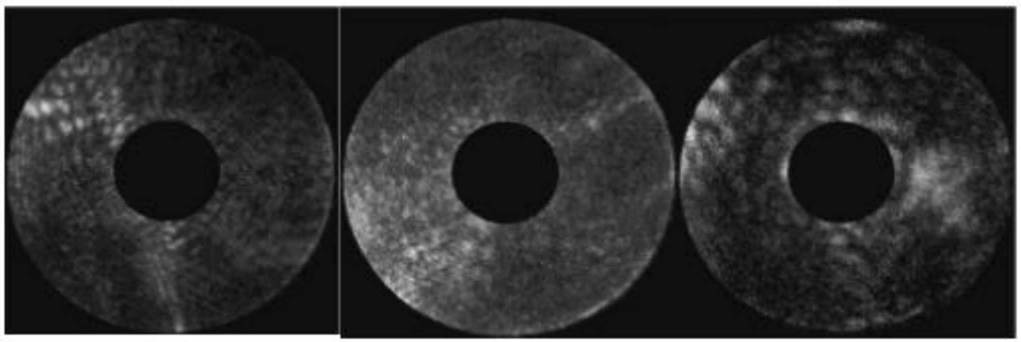

mixed phase

The majority of mid-latitude ice particles observed so far have been highly rough or complex.

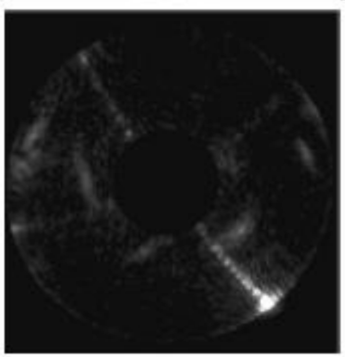

Smooth ice analogue

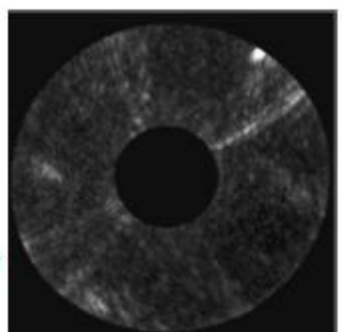

Rough ice analogue

Centre for Atmospheric & Instrumentation Research

AIITS – 2D patterns

TTL cirrus, 5 March 2015

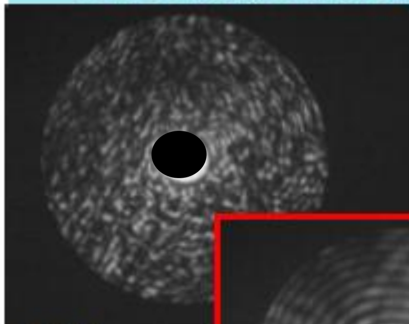

large
rough

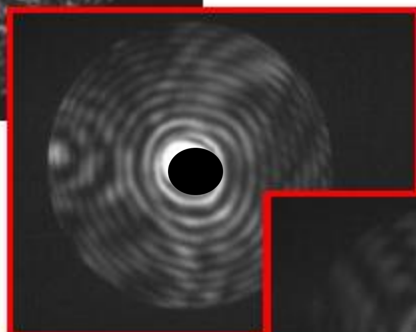

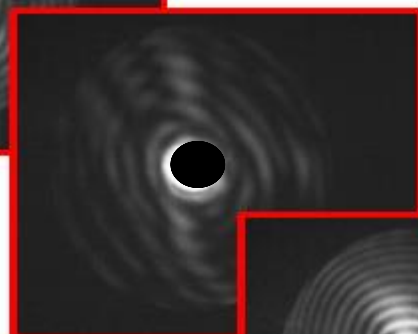

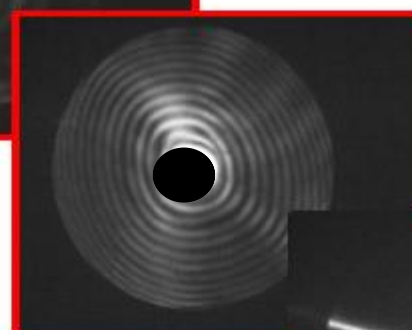

Lab data

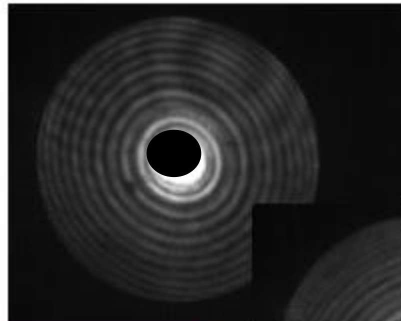

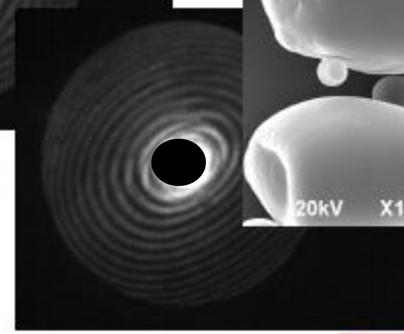

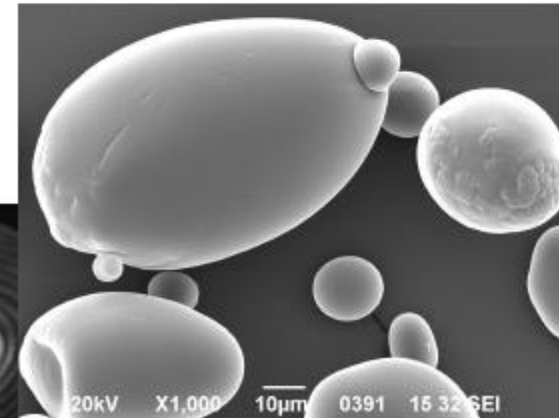

Ellipsoids, quasi-ellipsoids and "rounded polyhedra"?

TTL cirrus very different from temperate cirrus!

New analysis methods had be developed.

What is the nature of these particles?

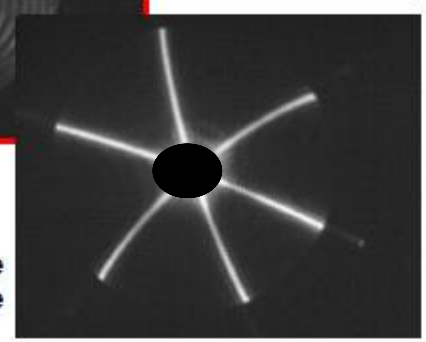

large
plate

Centre for Atmospheric & Instrumentation Research

So far one TTL cirrus case

CAST – AIITS data: rounded particles

TTL cirrus, 5 March 2015

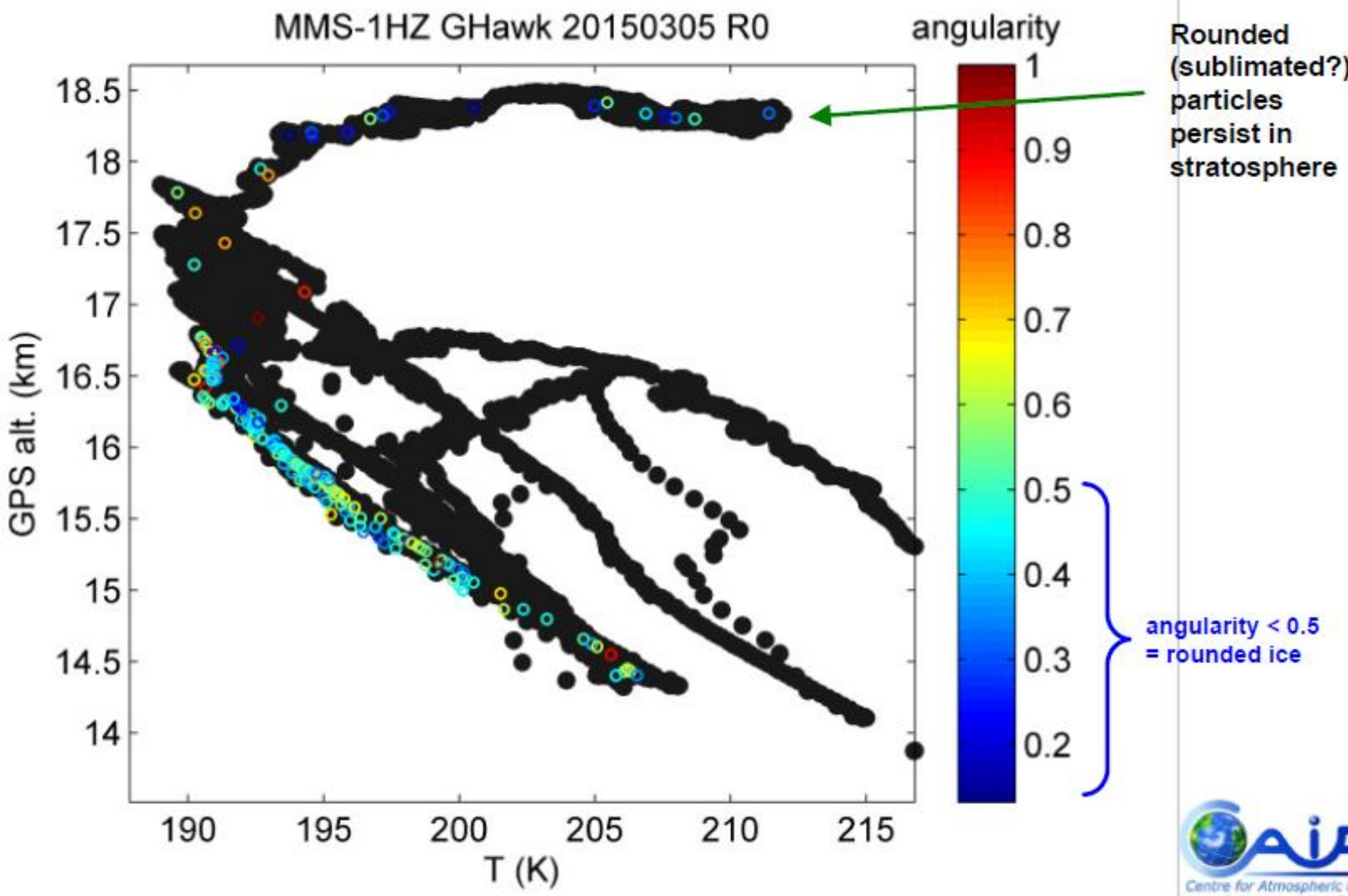

Discussion

We find that an ice optical parametrisation, based on the couple between q_i and T_c, improves model performance relative to an inconsistent scheme.

The ice optics assumes the same mass-D relationship and PSDs as used in the microphysics scheme. Thus, the same mass of ice is carried between the two schemes.

This allows direct comparison between a model prognostic variable and radiative measurements. These radiative measurements need to cover without gaps, the spectrum of importance to the energy of the earth's atmosphere.

Need predictive ice crystal aggregation schemes that are related to temperature rather than contrived realisations.

The uncertainty in the small ice mode of the ice crystal PSD needs to be substantially reduced as this ice mode has important implications for far-ir information content studies.

Therefore, require simulations that considers both possibilities of small ice representation.

New observations from the TTL might be suggesting that microphysics and radiative properties are completely different from temperate latitudes

Extra slides

Derivation of ensemble short-wave and long-wave single-scattering properties

- Short-wave: Assume geometric optics approximation: Apply Monte-Carlo Ray-tracing Method (Macke et al. 1996) to compute scattering phase matrix & total optical properties

Each element of the ensemble is **randomised** by **distortion** of the ray paths after each reflection/refraction event **and inclusions, assuming spherical air bubbles to mimic multiple-scattering between inclusions within each ice crystal element**

Each ensemble member is randomized from zero (pristine ice crystals) to fully randomized (distortions plus inclusions have been applied)

Long-Wave: Electromagnetic theory applied (T-matrix, Mischenko & Travis, 1998) + asymptotic approximation (Baran 2003).

The single-scattering properties properties are then integrated over the F07 tropical PSDs, as a function of IWC and $T_{c,}$ to predict the bulk scattering properties

Combine radar and lidar to obtain cloud profiles (DARDAR) to obtain ensemble weightings and global radiometric equivalent brightness temperatures **(Vidot et al., 2015 JGR, 120, doi:10.1002/2015JD023462)**

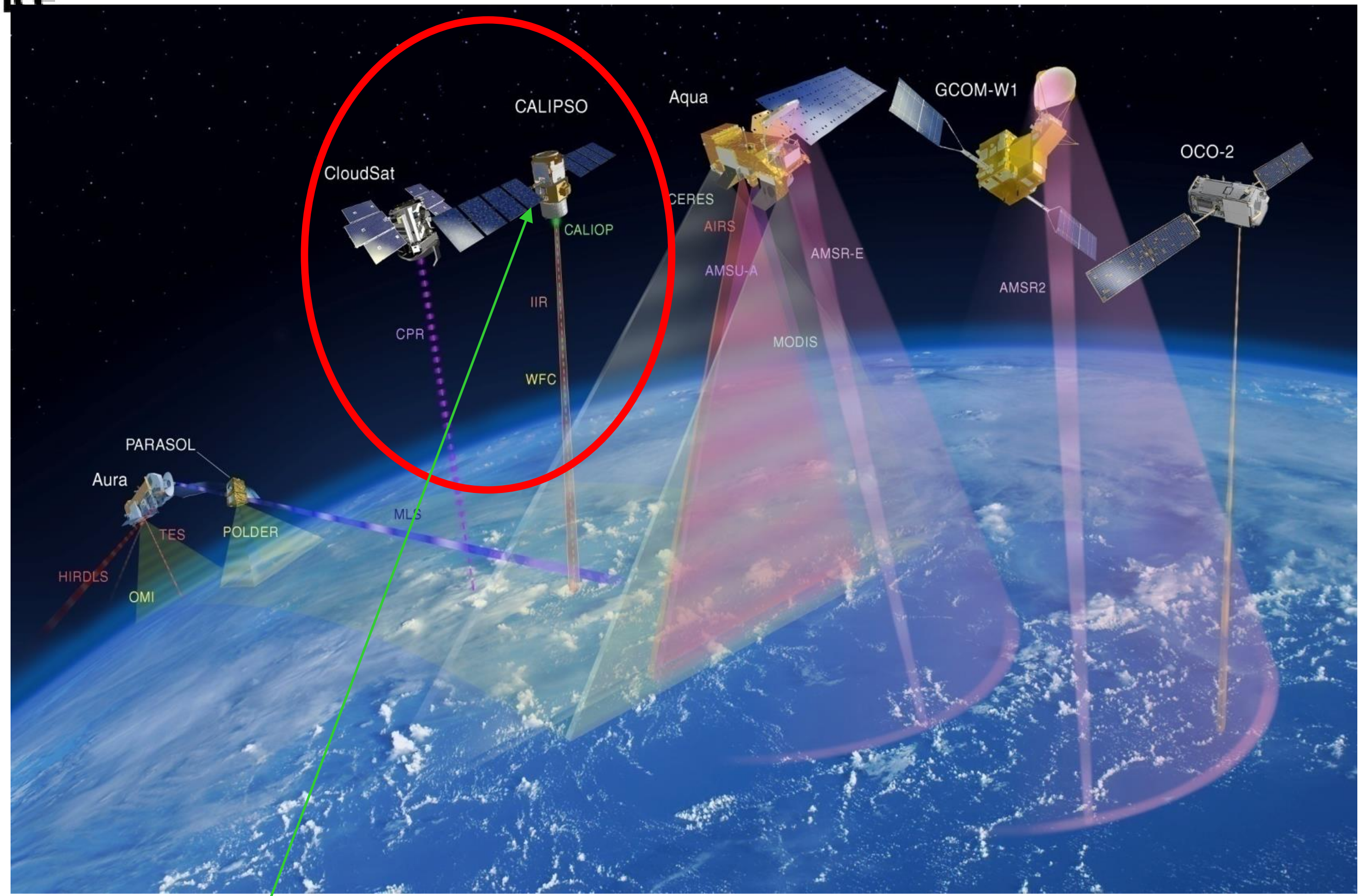

IIR centred at 8, 11 and 12 μm

An RTTOV example

Cloud profiles of IWC from DARDAR product

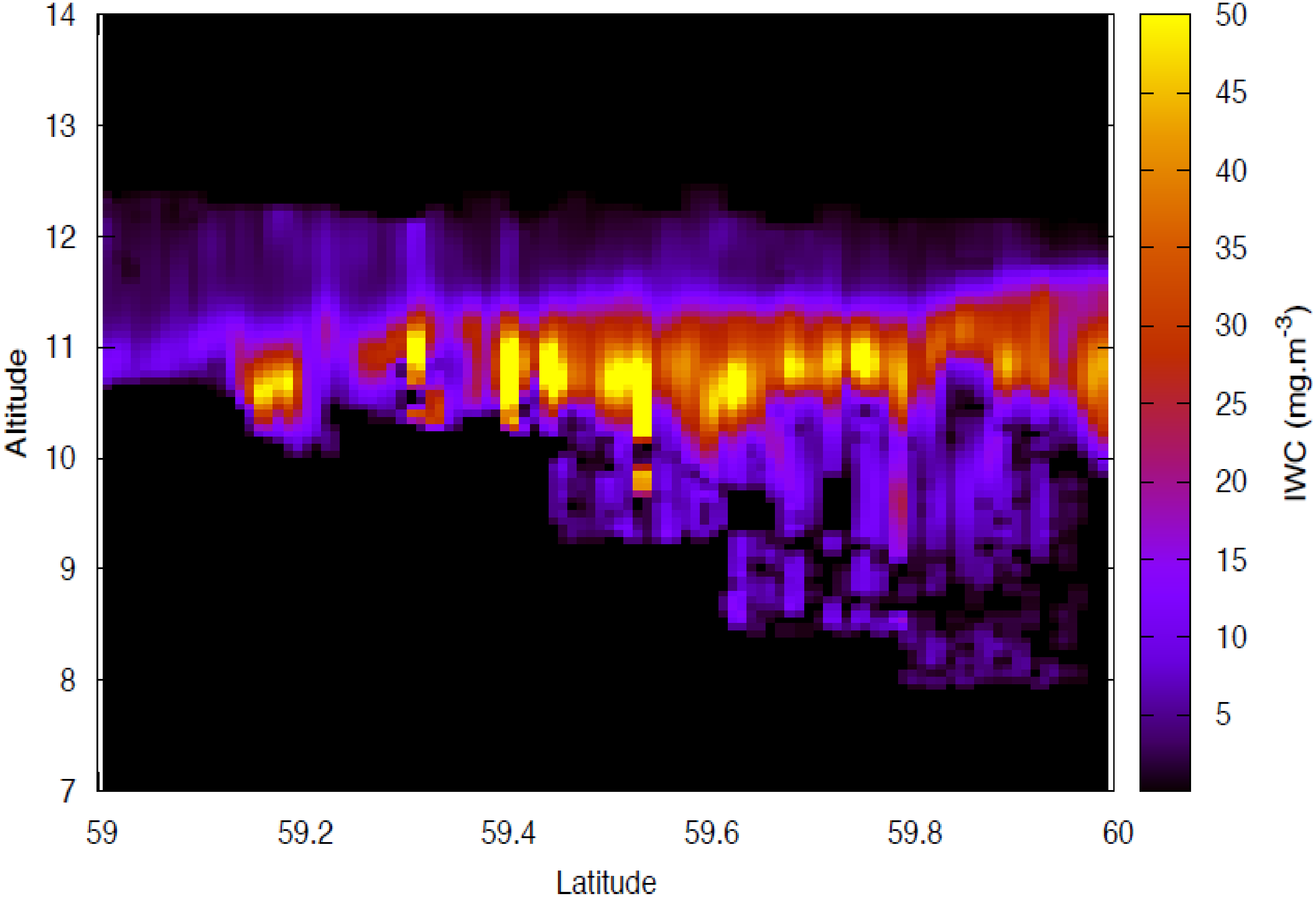

Global distribution of cirrus cases

N=26791

0.03 <τ **<4 Semi-transparent cirrus**

Altitudes high troposphere to stratosphere

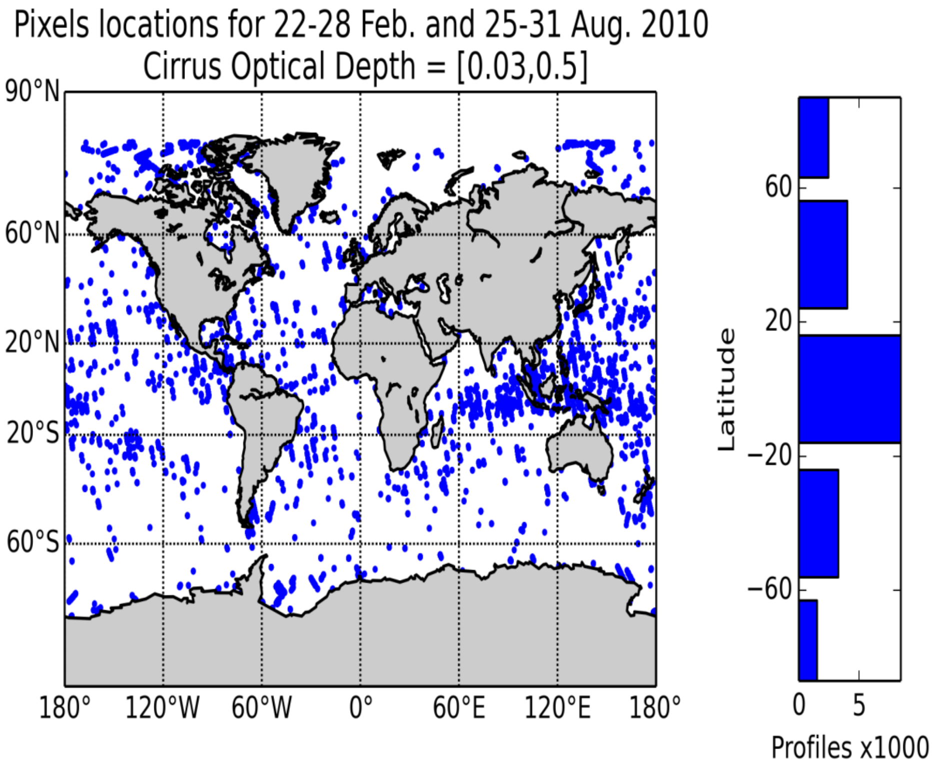

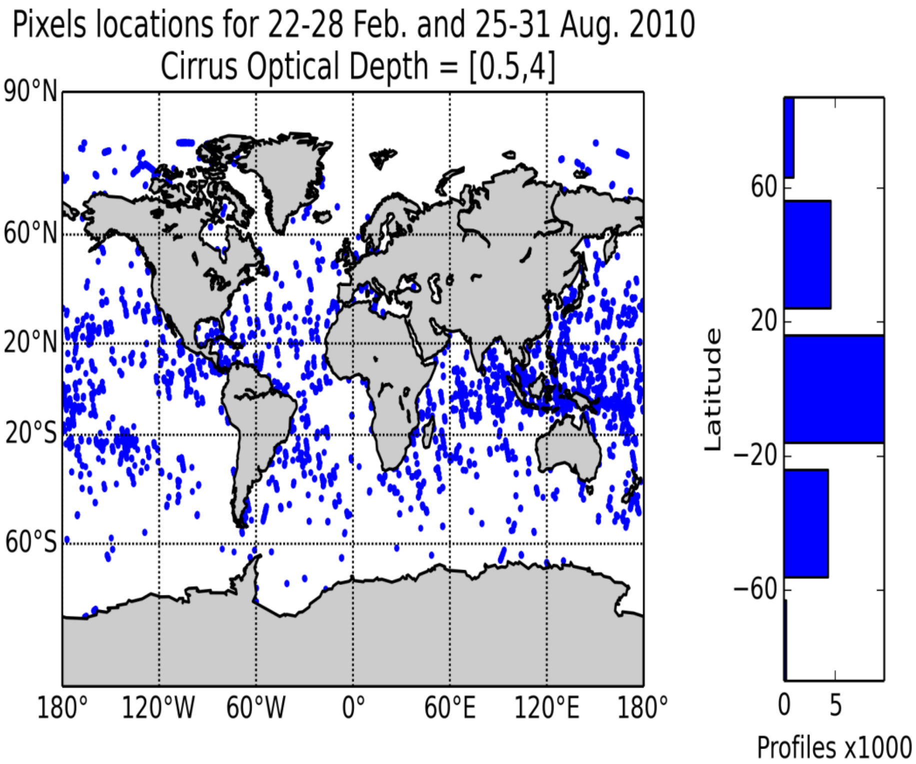

Results

Measurements - simulations

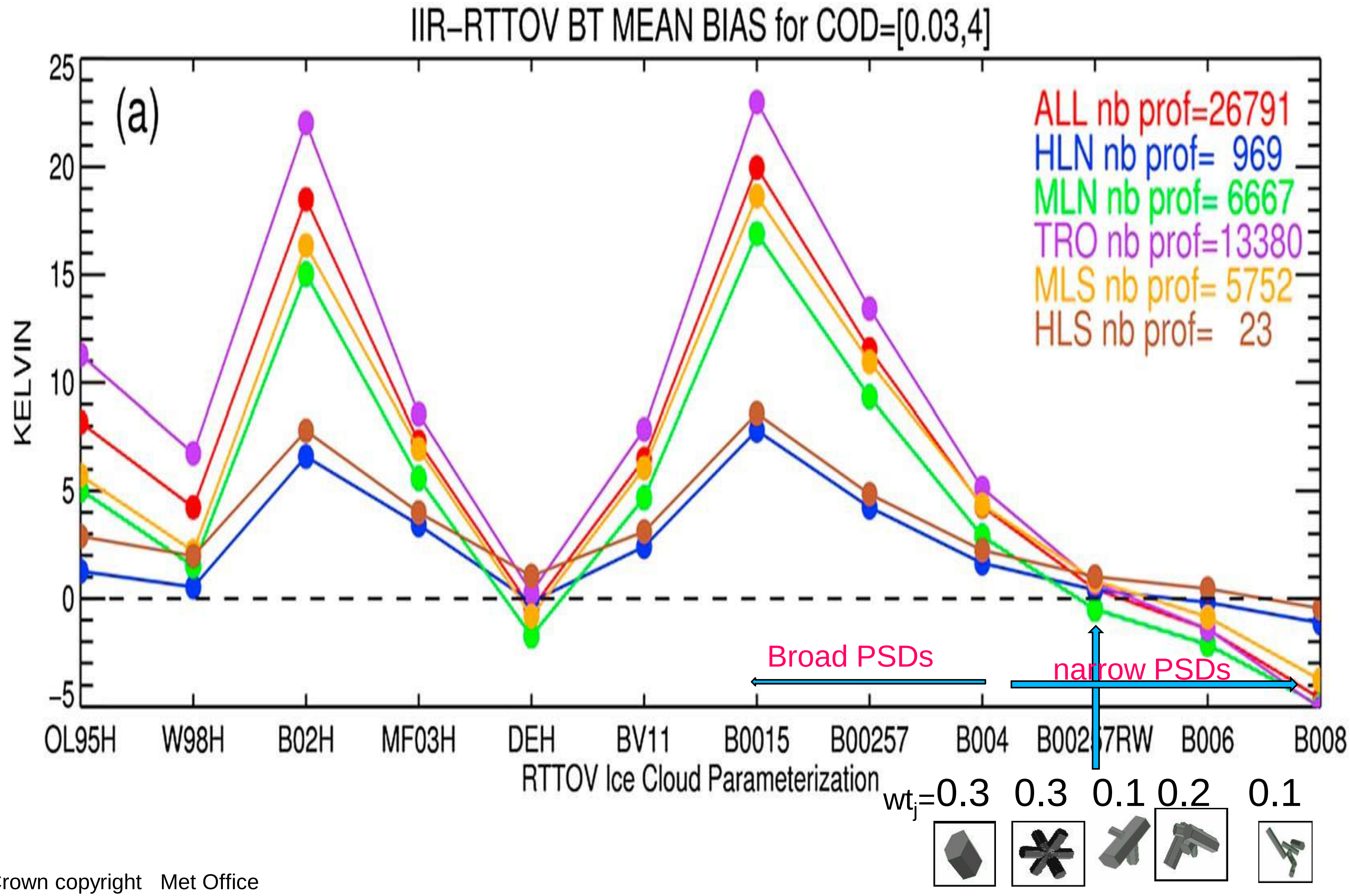

Microphysical Consistency

Observed area Relationships: Area ratio:

$A(D)/A_c(D)$

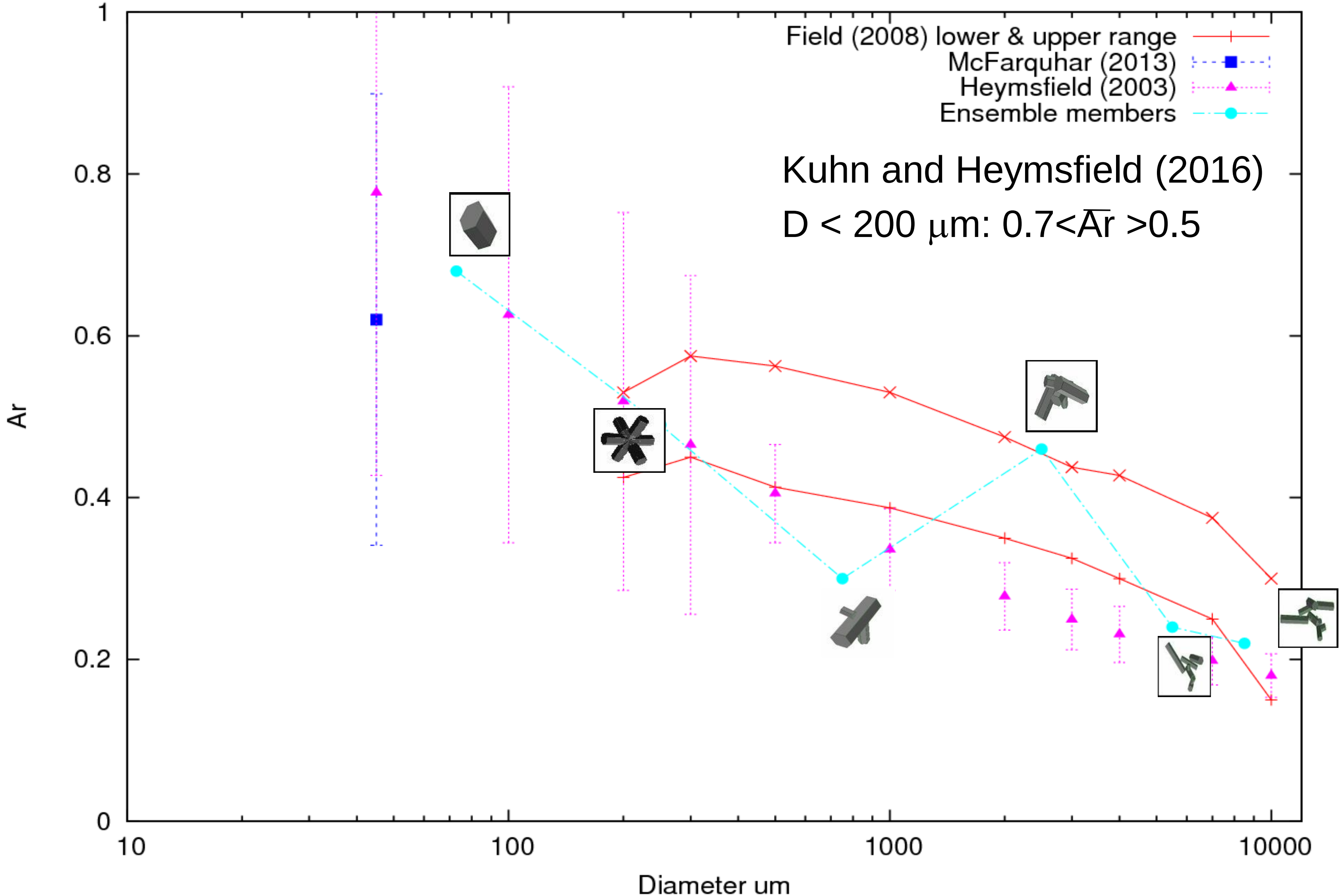

Edwards et al., (2007), Ice crystal model - the moderately surface roughened eight-branched hexagonal aggregate (Yang & Liou, 1997)

Met Office

$\omega_0(D_e), g(D_e), K_{ext}(q_i, D_e); D_e(T_c)$

Prognostic variable in microphysics

Diagnosed variable **in radiation**

$$D_e = 3/2 \int m(\underline{q})\, n(\underline{q})\, d\underline{q} / \rho_I \int \langle S(\underline{q}) \rangle\, n(\underline{q})\, d\underline{q}$$

Foot (1988)

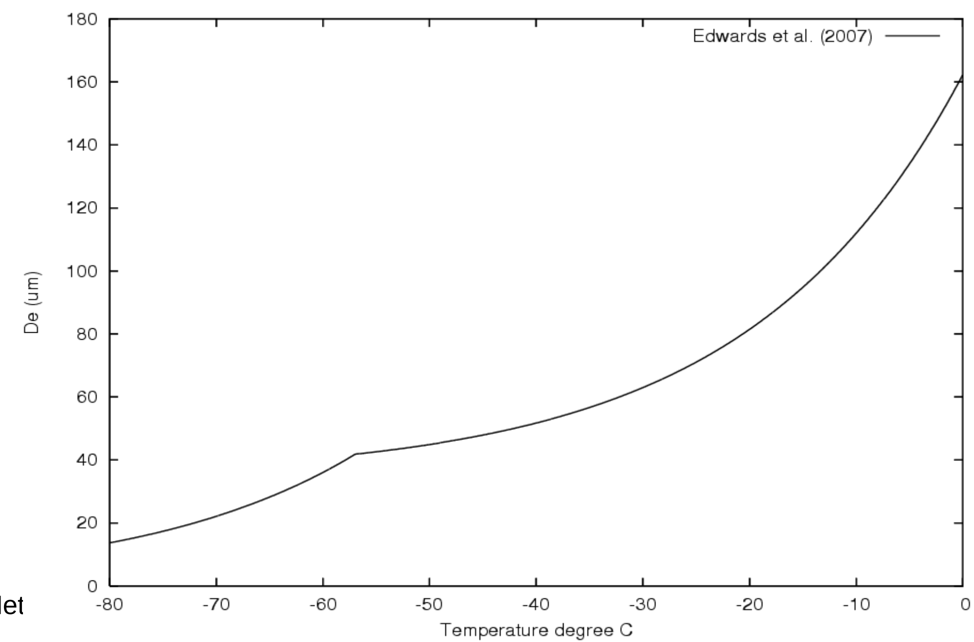

Edwards et al., (2007), Ice crystal model - the moderately surface roughened eight-branched hexagonal aggregate (Yang & Liou, 1997)

$\omega_0(D_e), g(D_e), K_{ext}(q_i, D_e); D_e(T_c)$

Prognostic variable in microphysics

Diagnosed variable **in radiation**

$$D_e = 3/2 \int m(\underline{q})\, n(\underline{q})\, d\underline{q} / \rho_I \int \langle S(\underline{q}) \rangle\, n(\underline{q})\, d\underline{q}$$ Foot (1988)

Sieron et al, 2017 [JGR, 122,7027-7046]Microwave simulations at 91.665 GHz

Table 1. Scattering Optical Depths and Brightness Temperatures Output From CRTM Simulations With the Same Water Content, Effective Radius, and Particle Properties but With Different Particle Size Distributions[a]

			Monodisperse		Exponential	
Effective Radius (microns)	$\tau_s m/\tau_s exp$	Water Content (g m^{-3})	Scattering Optical Depth	Brightness Temperature (K)	Scattering Optical Depth	Brightness Temperature (K)
0		0	0	276.18	0	276.18
103.7	4.32	1.15×10^{-4}	4.03×10^{-6}	272.96	1.74×10^{-5}	272.96
184.3	3.92	1.15×10^{-3}	2.24×10^{-4}	272.91	8.79×10^{-4}	272.79
327.8	2.88	1.15×10^{-2}	1.21×10^{-2}	270.57	3.49×10^{-2}	267.94
582.9	1.81	1.15×10^{-1}	5.54×10^{-1}	204.09	$1.00 \times 10^{+0}$	200.35
1037	1.77	$1.15 \times 10^{+0}$	$1.16 \times 10^{+1}$	75.57	$2.05 \times 10^{+1}$	74.74

$D_e = 3/2 \int m(D)\, n(D)\, dD / \rho_I \int \langle S(D) \rangle\, n(D)\, dD$

Let us assume a cloud of ice in which the ice crystals become aggregated after about 200 μm (Schmitt & Heymsfield, 2010) $\langle S(D) \rangle = cD^{1.76}$, let us assume that these ice crystals have $m(D)=0.0257D^2$ (Cotton et al., 2013). At sizes less than this, we assume ρ=700 kg m^{-3} and $\langle S(D) \rangle = kD^{1.86}$ (Kuhn and Heymsfield, 2016). Apply these mass- and area-dimension relations to D_e integrated over 20662 PSDs, the normalised PDF of D_e for such a simulation is:

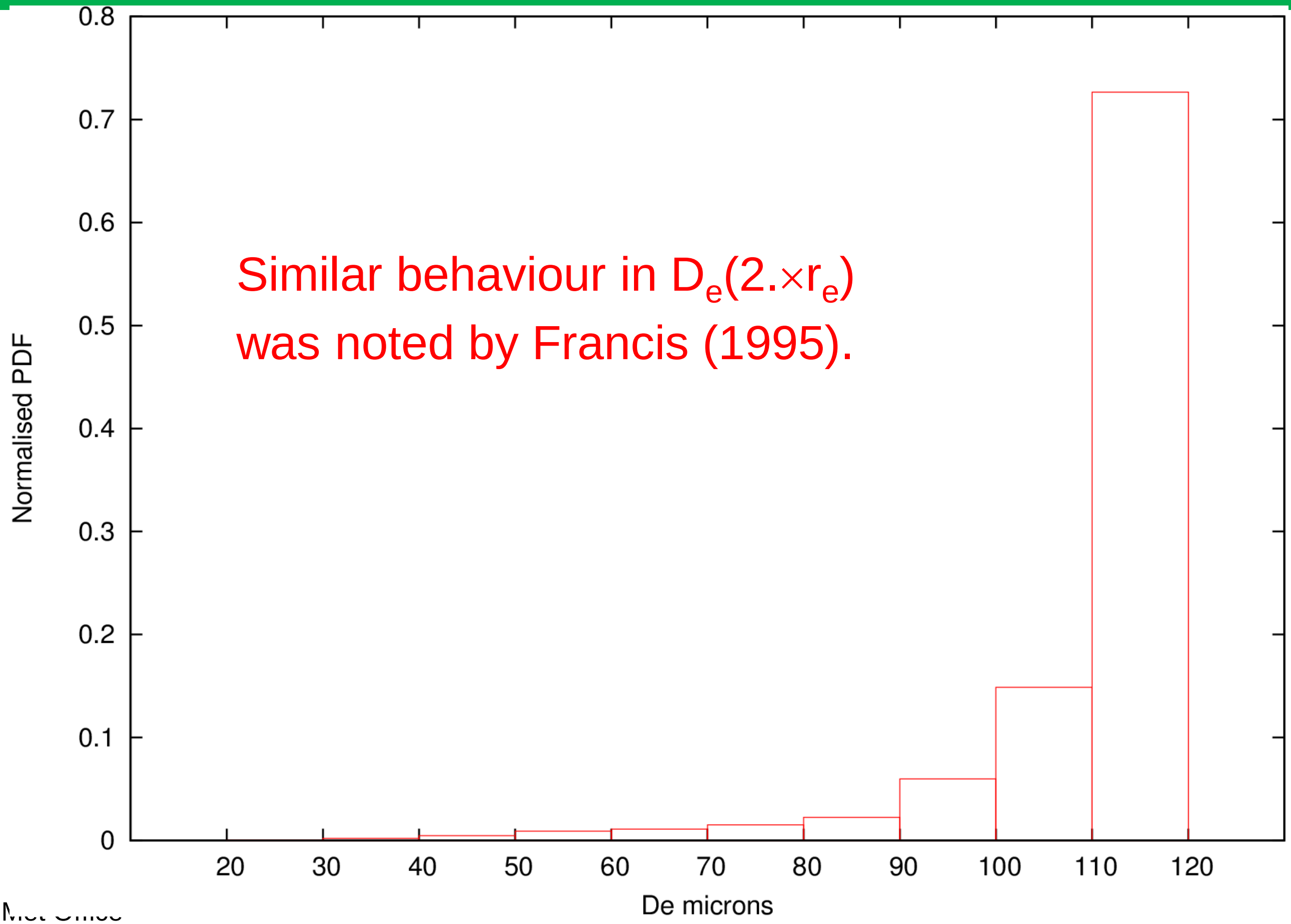

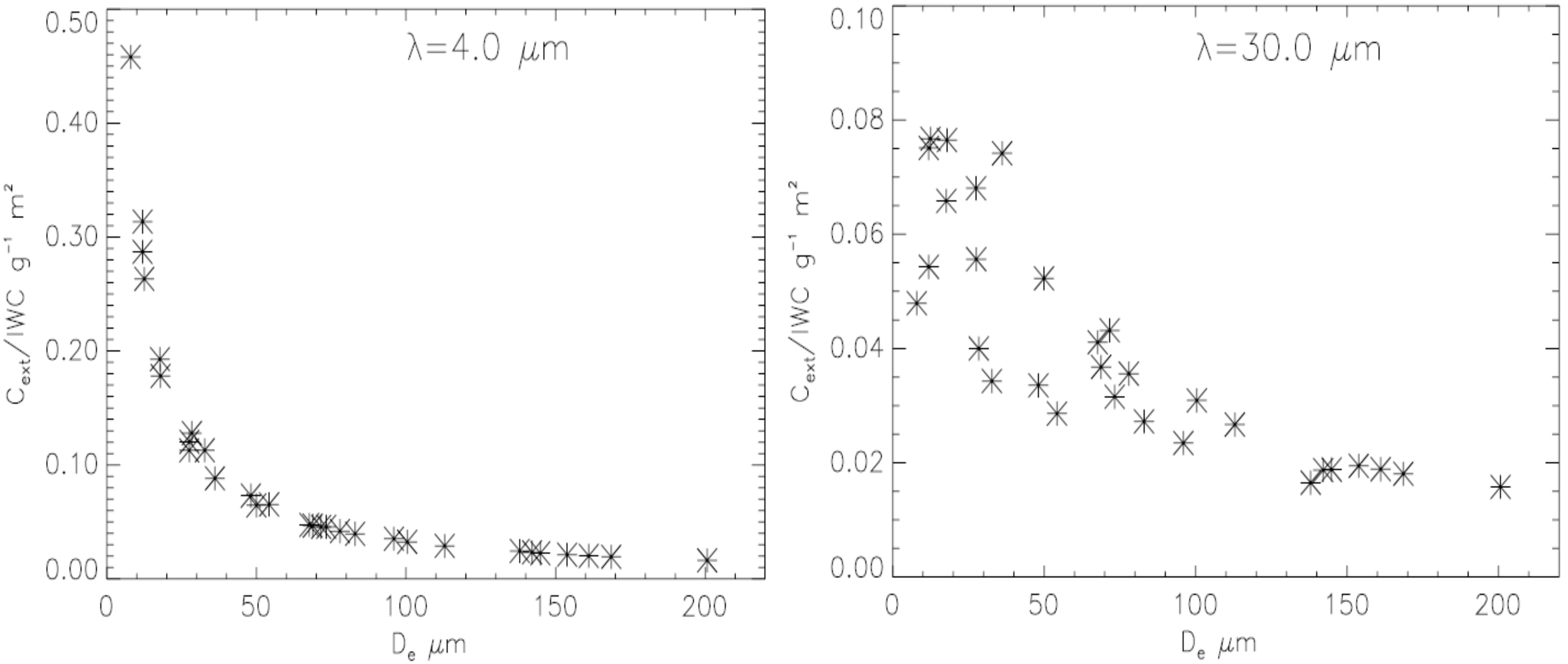

Baran, 2005 [QJRMS, 131, 1129-1142]

See also Sieron et al. (2017), JGR, 122,7027-7046

The concept of an effective diameter

Met Office

Given a shape distribution of non-spherical particles how best is it to define the size of that shape distribution ? (Foot, 1988)

$D \gg \lambda$

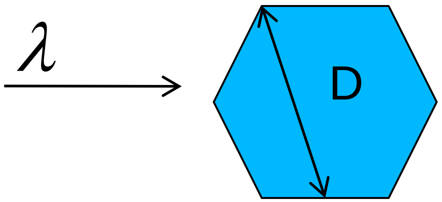

$$d_e = \frac{volume}{projected-area}$$

'Effective distance' (Bryant and Latimer, 1969; Mitchell & Arnott al., 1994…)

Over a PSD of equivalent spheres

$$d_e = \frac{4}{3} r_e$$

$$D_e = \frac{3}{2} \frac{Mass}{\rho_i (projected - area)}$$

'Effective diameter'

Require PSDs: we use moment parametrisation by Field et al., (2007)

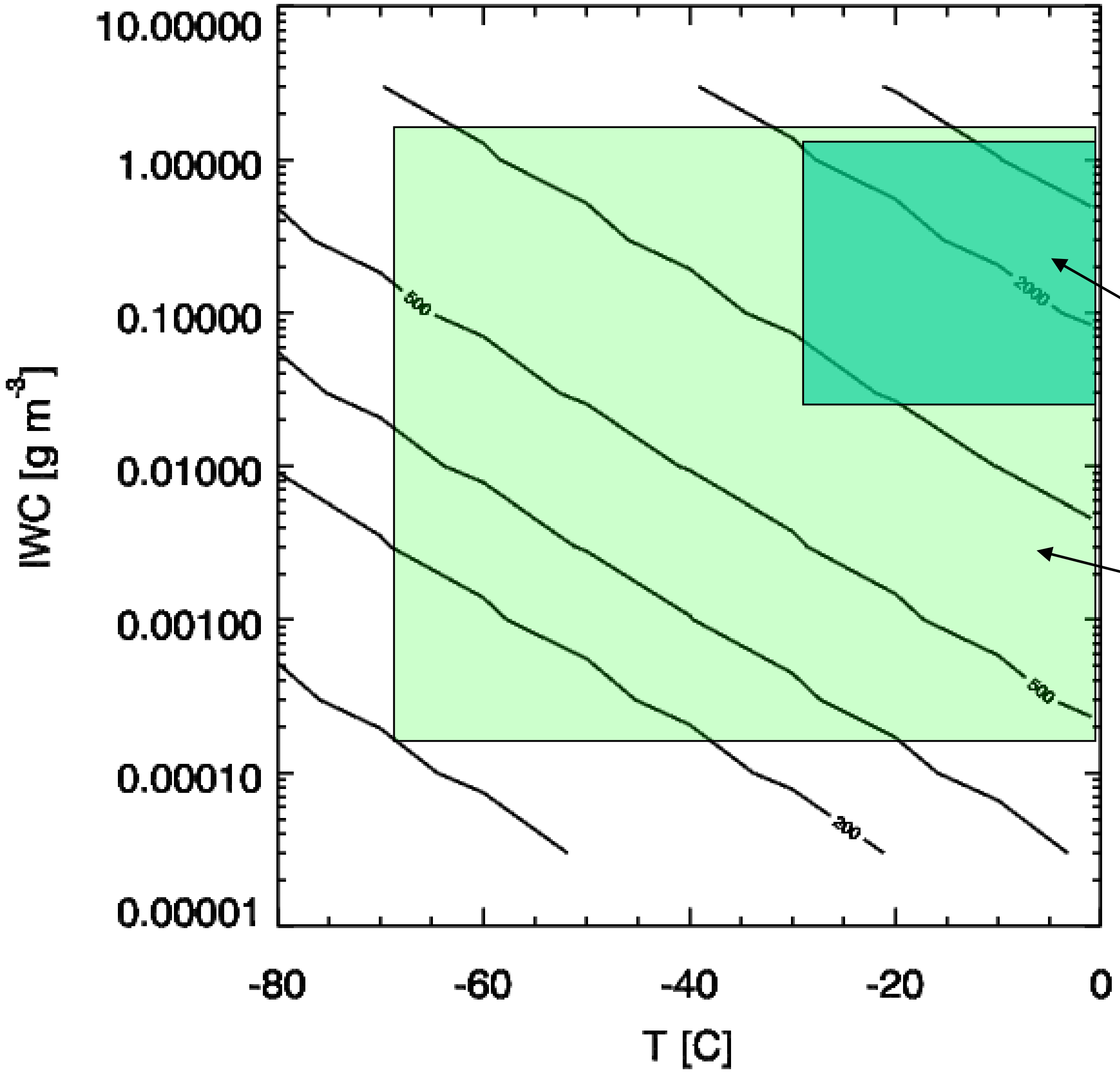

Houze et al. 1979

39 in-situ PSDs (current PSD assumption in global operational model, where PSD shape is kept constant At temperatures < -30^{o}C)

Field et al. 2007

10000 in-situ measurements obtained in tropics and mid-latitudes.

Met Office

The parametrisation

$K_{ext}(\lambda_{E\text{-}S},q_i,T_c) = a_\lambda(q_i / T^4)$; $\omega_0(\lambda_{E\text{-}S},q_i,T_c) = b_\lambda + c_\lambda q_i T$

$g(\lambda_{E\text{-}S},q_i,T_c) = d_\lambda + e_\lambda q_i T$

If $q_i > 10^{-3}$ kg/kg, then

$\omega_0 = \omega_0(q_i = 10^{-3}$ kg/kg)

$g = g(q_i = 10^{-3}$ kg/kg)

Relative % errors in the K_{ext} and g parametrisations at E-S(SW B5 1.19-2.38 μm)

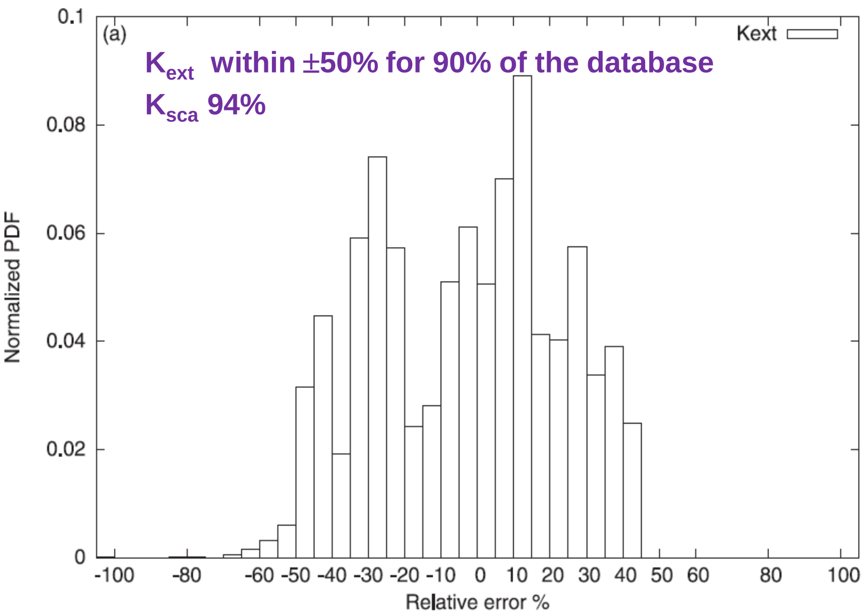

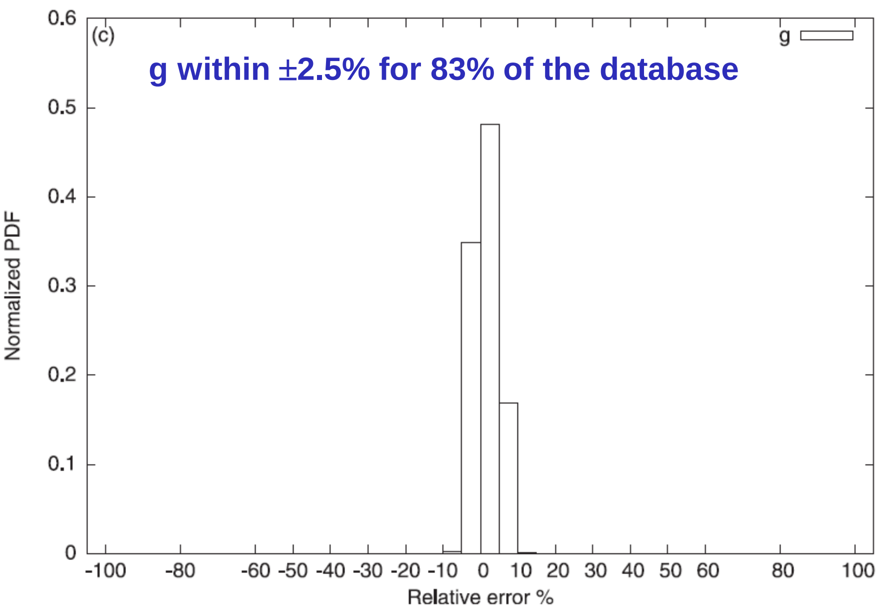

Boundary Element Method

- also known as Method of Moments
- reformulate the problem as integral equations on the boundary Γ
- solve the problem on the boundary Γ
- extend the solution to the interior/exterior by representation formulae (Stratton - Chu)
- assumption: piecewise homogeneous media

Why the Boundary Element Method

- lower dimensional manifold to discretize
- automatically incorporates outgoing behaviour at infinity
- flexibility with geometry; it can handle complex ice crystal shapes

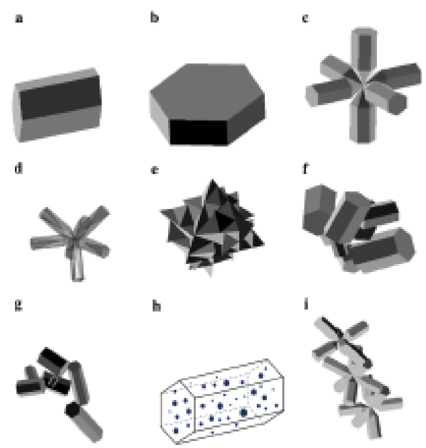

Ice models. Taken from (Baran, 2012).

From Kleanthous, Betcke, Hewitt, Scroggs, Baran submited JQSRT 2018

- parameter values: $k_e = 12$, $n = 1.311 + 2.289 \times 10^{-9} i$ (weak absorption),

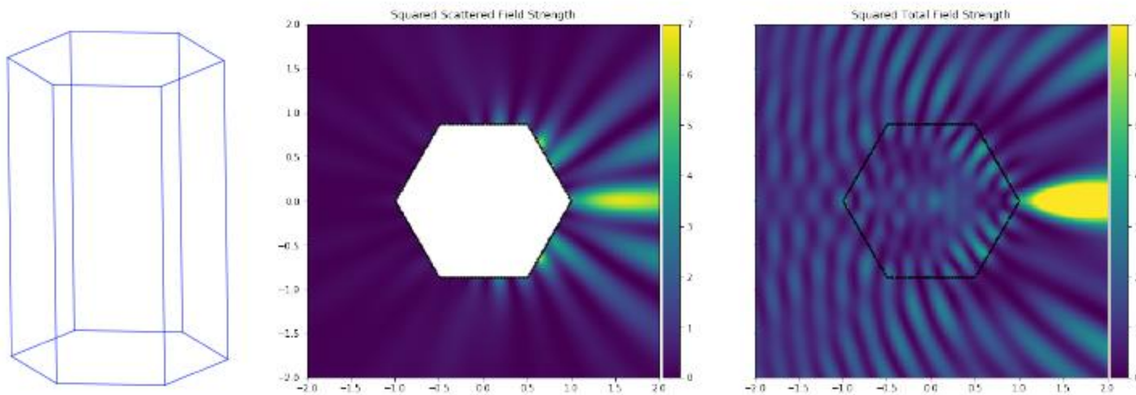

- parameter values: $k_e = 16$, $n = 1.2$, $k_i = 19.2$, $\mu_e = \mu_i = 1$, $h = 0.0628$

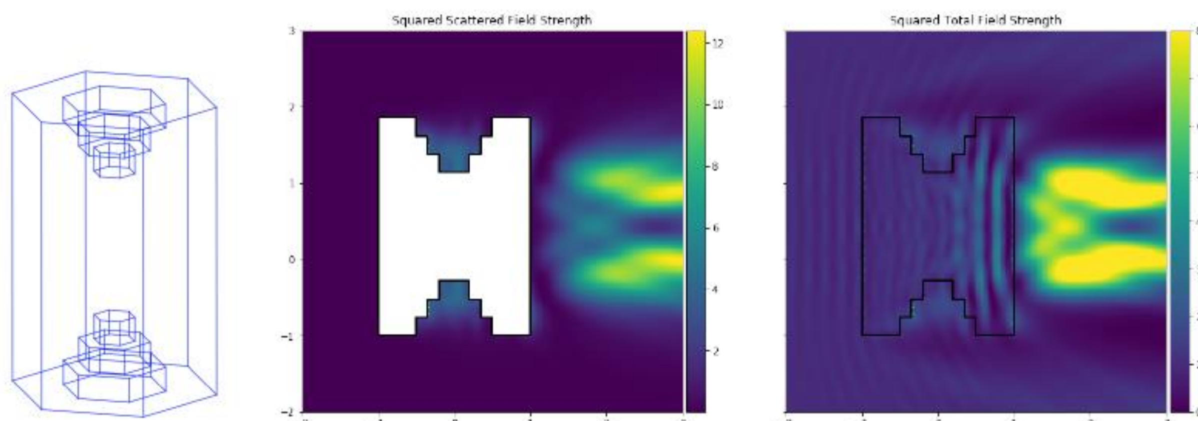

From Kleanthous, Betcke, Hewitt, Scroggs, Baran submited JQSRT 2018

X=120

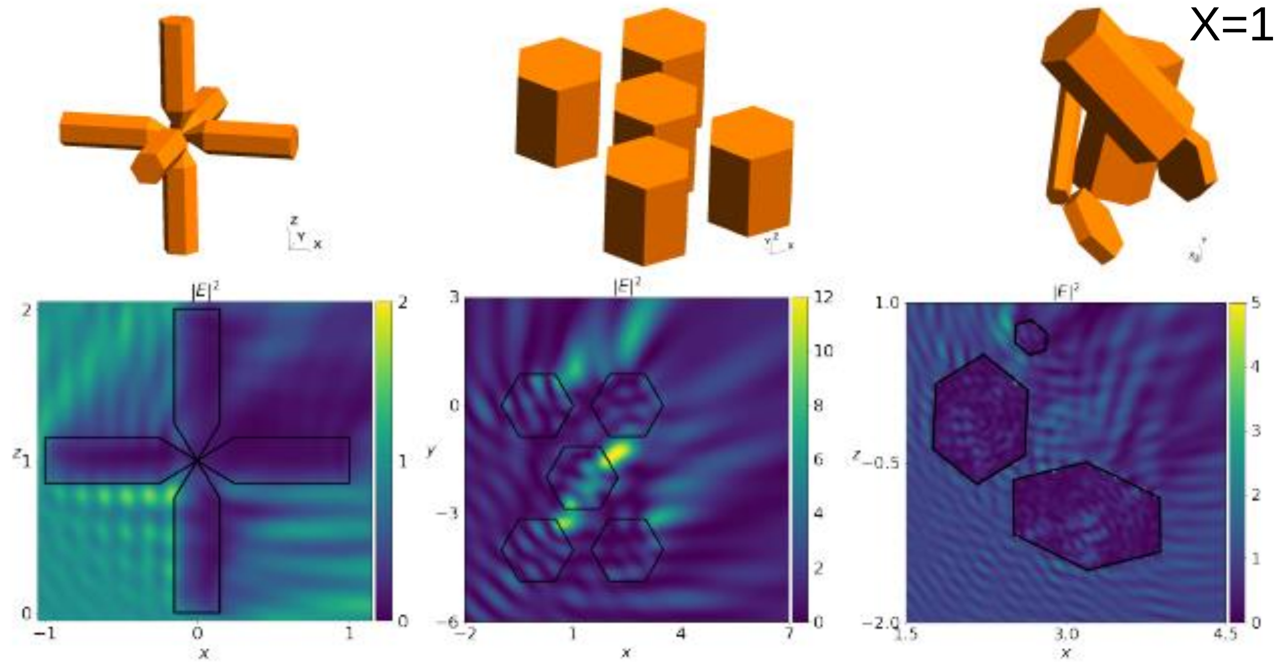

Figure 8: Squared magnitude $|\mathbf{E}|^2$ of the electric field for multiple scattering ($M > 1$) restricted to different planes. In the case of the bullet-rosette with 6 branches ($M = 6$) the incident wave is $\mathbf{E}^{inc}(\mathbf{x}) = \mathbf{p}e^{ik_e\mathbf{d}\cdot\mathbf{x}}$, with $\mathbf{d} = (\sqrt{3}/2, 0, 1/2)^T$ and $\mathbf{p} = (0, 1, 0)^T$, with $k_e = 25$, $n = 1.0833 + 0.204i$, $k_m = nk_e$, and $\mu_e = \mu_m = 1$, for $m = 1, \ldots, 6$. For the array of five hexagonal columns ($M = 5$) the incident wave is $\mathbf{E}^{inc}(\mathbf{x}) = \mathbf{p}e^{ik_e\mathbf{d}\cdot\mathbf{x}}$, with $\mathbf{d} = (1/\sqrt{2}, 1/\sqrt{2}, 0)$ and $\mathbf{p} = (0, 0, 1)^T$, with $k_e = 5$, $n = 1.311 + 2.289 \times 10^{-9}i$, $k_m = nk_e$, and $\mu_e = \mu_m = 1$, for $m = 1, \ldots, 5$. For the aggregate of randomly oriented hexagonal columns and plates ($M = 5$) the incident wave is $\mathbf{E}^{inc}(\mathbf{x}) = \mathbf{p}e^{ik_e\mathbf{d}\cdot\mathbf{x}}$, with $\mathbf{d} = (1/\sqrt{2}, 0, 1/\sqrt{2})$ and $\mathbf{p} = (0, 1, 0)^T$, with $k_e = 30$, $n = 1.311 + 2.289 \times 10^{-9}i$, $k_m = nk_e$, and $\mu_e = \mu_m = 1$, for $m = 1, \ldots, 5$. The diameter of the aggregate is 4 so that the size parameter is 120. The mesh size in all cases is $h = 2\pi/(10k_e)$.

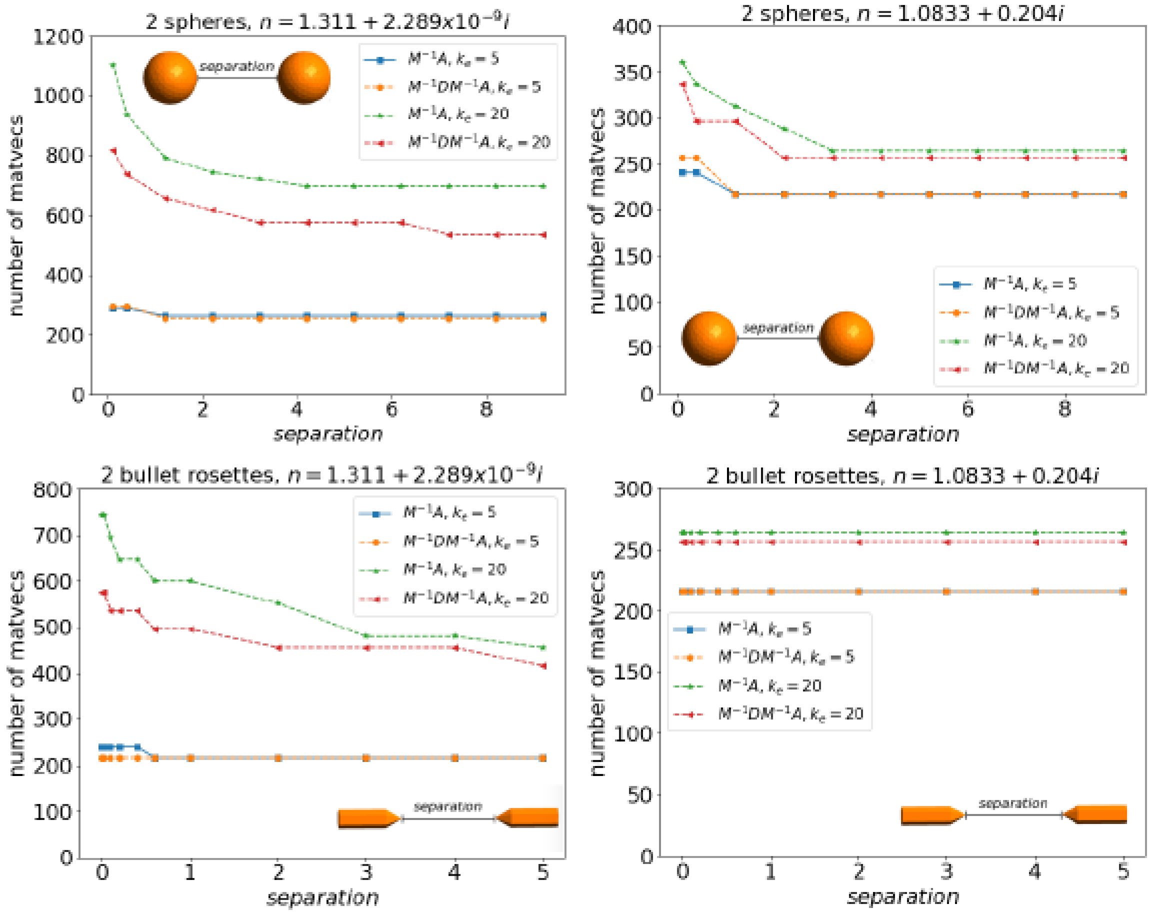

Figure 5: Number of matvecs for $\mathbf{M}^{-1}A$ and $\mathbf{M}^{-1}\mathbf{D}\mathbf{M}^{-1}\mathbf{A}$ for multiple scattering by a pair of identical scatterers as a function of their separation. Results are shown for two spheres of radius 0.4, and for two branches of a bullet rosette. In each case we consider two values of k_e and two refractive indices $n_1 = 1.0833 + 0.204i$ and $n_2 = 1.311 + 2.289 \times 10^{-9}i$. Other parameters are as in Table 3.

8.50 µm

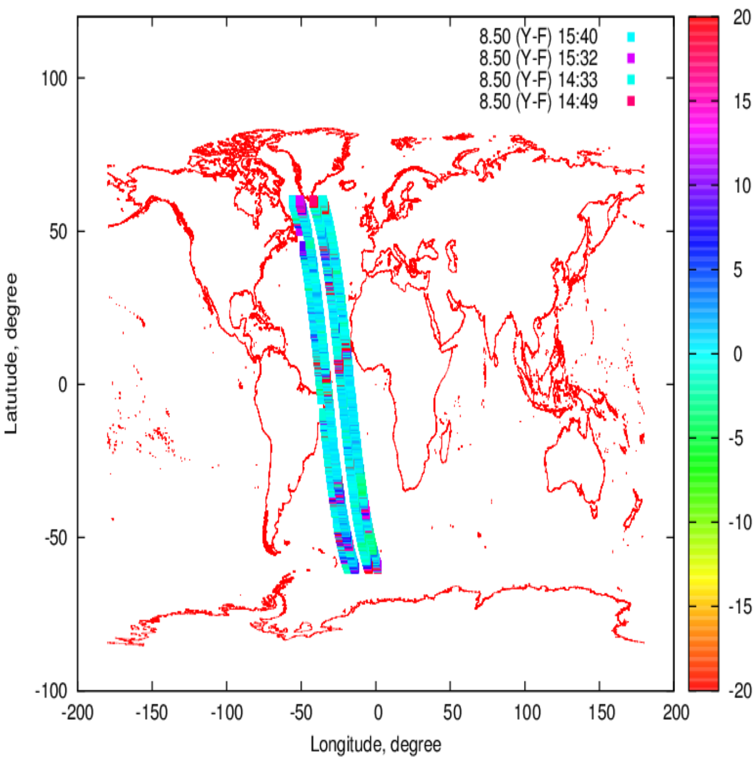

10.60 µm

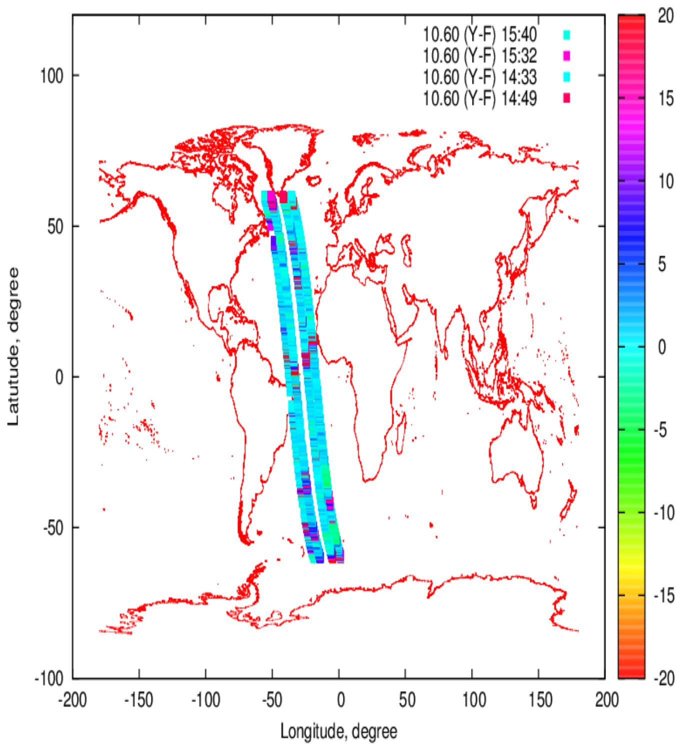

12.09 μm

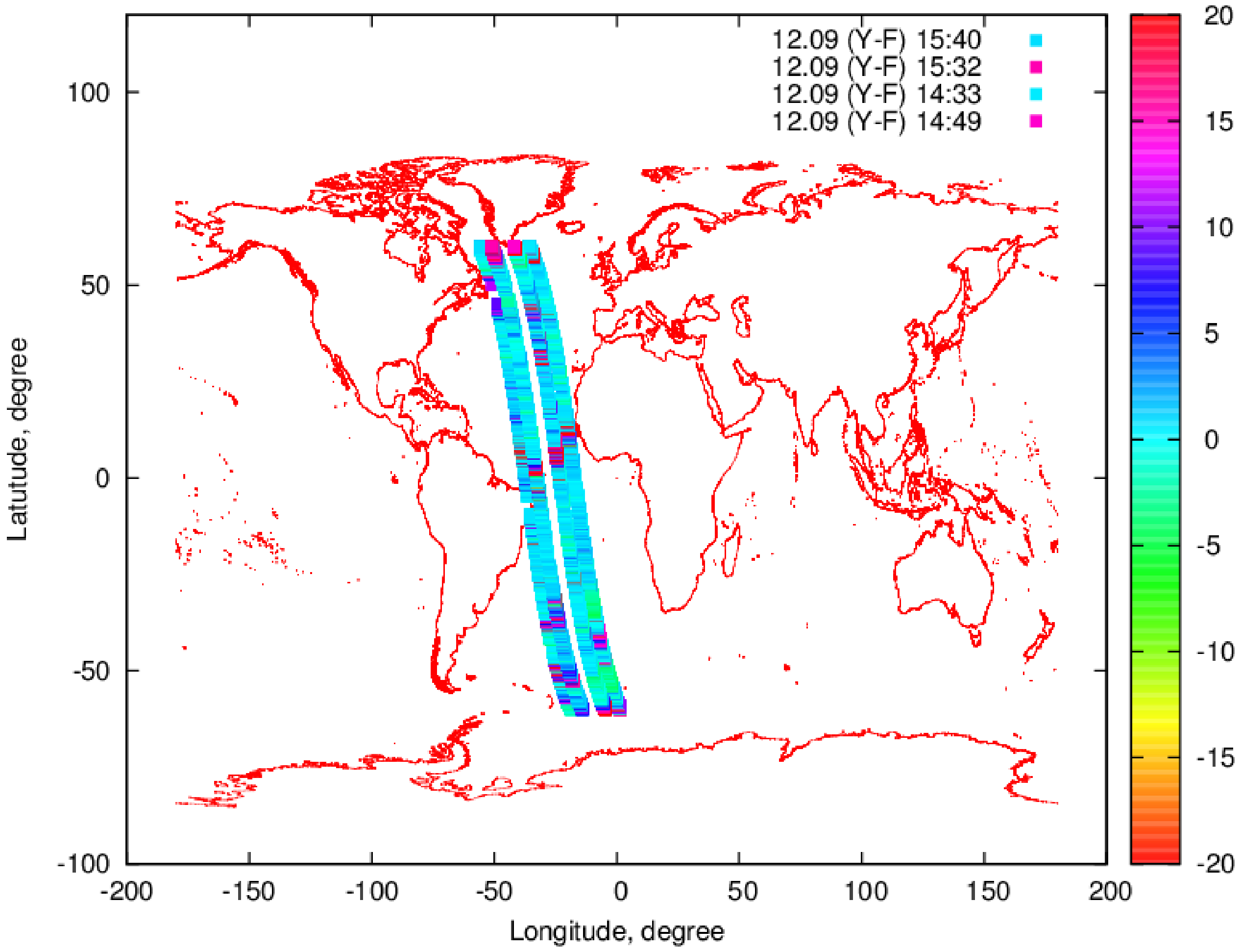
12.09 (Y-F) 15:40
12.09 (Y-F) 15:32
12.09 (Y-F) 14:33
12.09 (Y-F) 14:49
Latutude, degree
Longitude, degree
100
50
0
-50
-100
-200
-150
-100
-50
0
50
100
150
200
20
15
10
5
0
-5
-10
-15
-20

Furtado et al. 2015

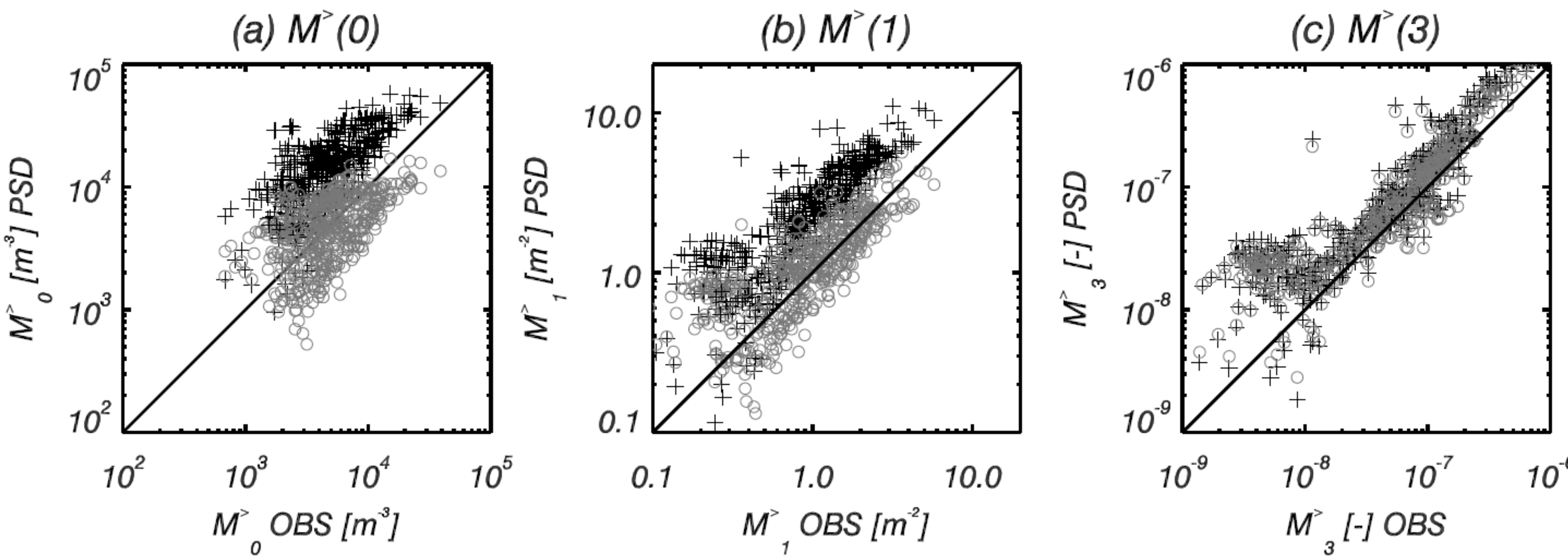

+ Houze et al. 1979

○ Field et al. 2007

Mid-latitude anvil cloud

Near cloud-top

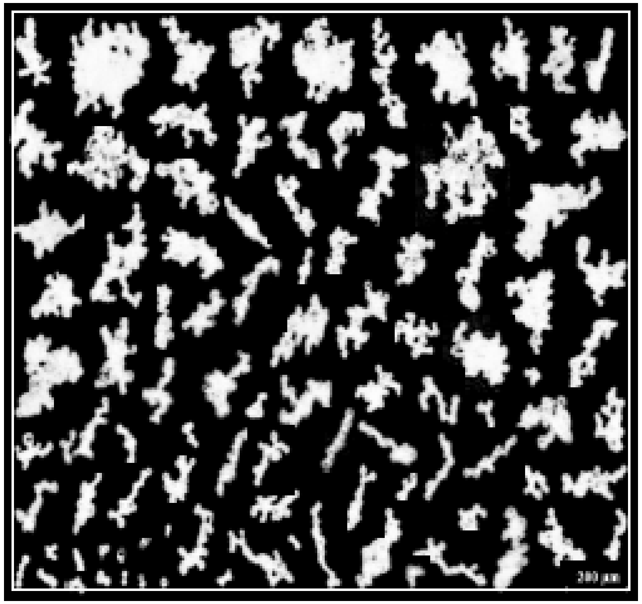

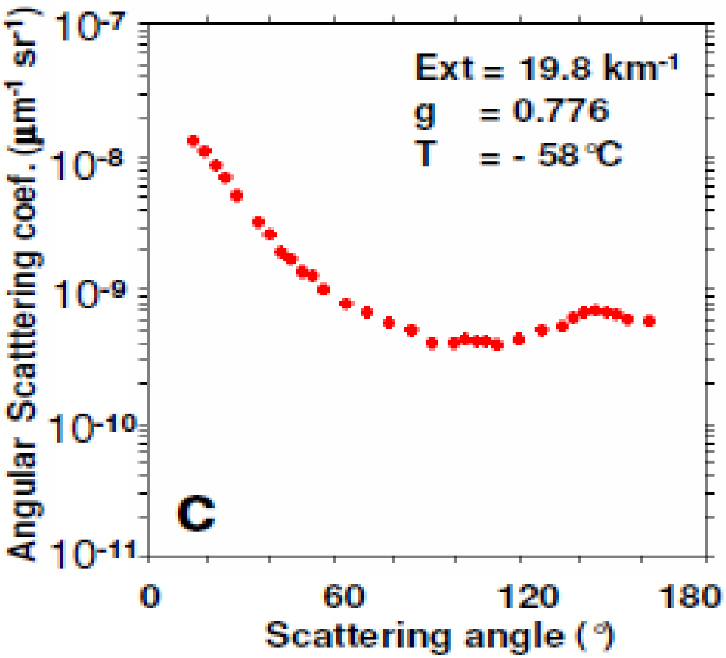

g=0.776 ±5%

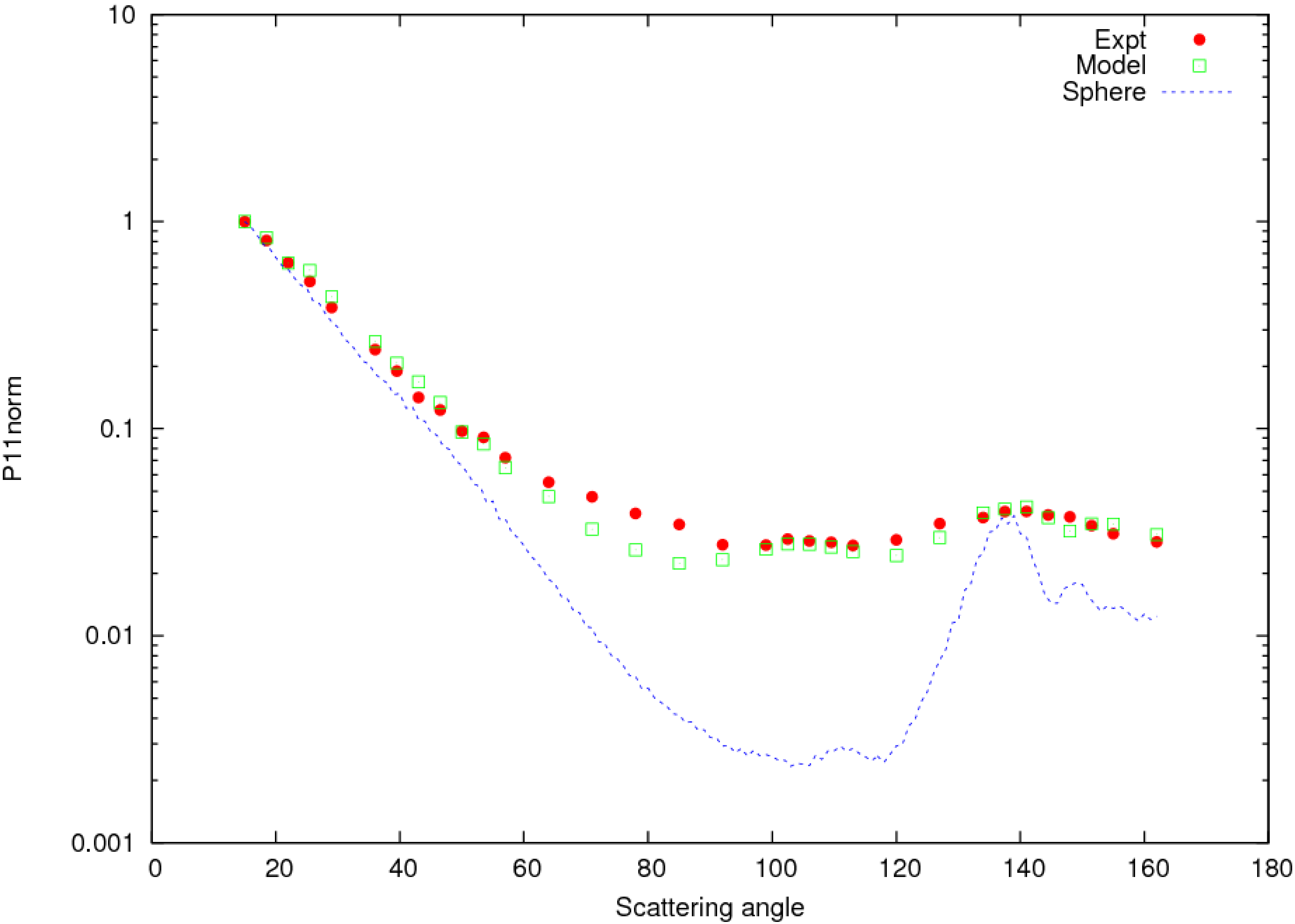

10
1
0.1
0.01
0.001
P11norm
0
20
40
60
80
100
120
140
160
180
Scattering angle
Expt
Model
Sphere

Instrument Background : POLDER

CNES/LOA instrument, Parasol launched Dec. 2004 - 2015

Sensor Characteristics

- 10 spectral bands ranging from 0.443 to 1.020 μm
- Multidirectionnal observations (up to 16 directions)
- Spatial resolution : 6x7 km

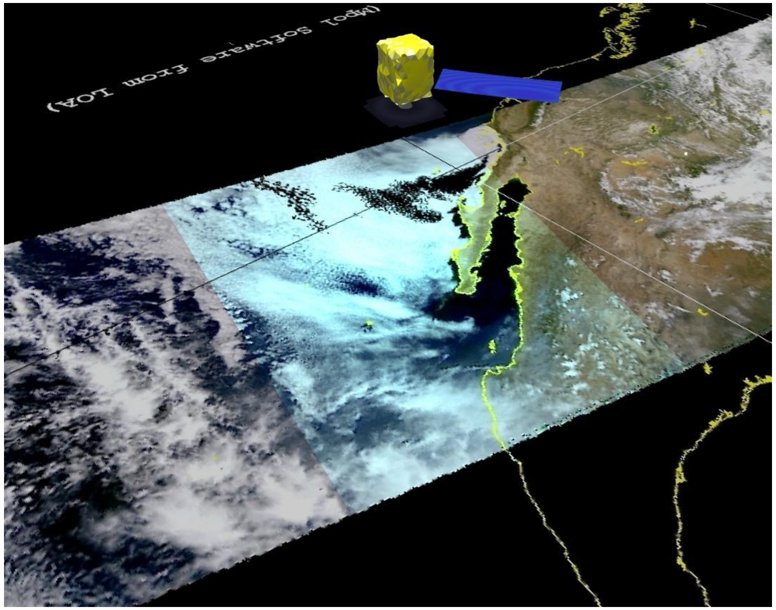

The ice optics: The SW

POLDER-3 global test of various model phase functions

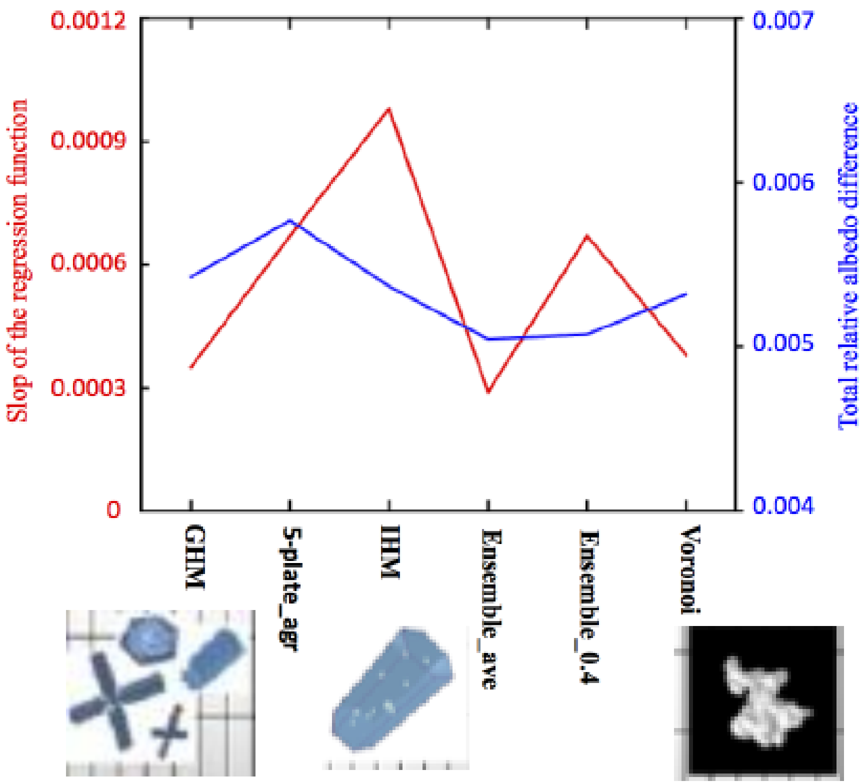

Pixels~600000 (14x600000~9 M angles)
20-22 March, June, Sept, Dec
Most obs obtained between latitudes

Roughened ice crystals best minimise differences between measurements & models. The ensemble model generally provides the better fit to the measurements.

From Letu et al., 2016: ACP, 16, 12287-12303

Single-layer direct IWP retrievals at 0.85. 2.13, 8.6, 10.6, 12.0 µm (IIR+MODIS) from Sourdeval et al., 2016, QJRMS, 142, 3063-3081